between the AE entry rates per month was performed pre and post implementation.
Results: There was an overall reduction from 254 dictionary terms to 63 terms. With the branching subcategory display, the effective number of terms that the end user has to sort through decreased from 254 to between 8 and 14 options. AE entry rates were measured pre and post implementation and illustrated in Table 1. The comparison of the two time periods showed a very dramatic increase of the recording of "defects" post implementation. Overall, there was a 124.4% increase when the two time periods were compared.

Table 1.

Month	Usage PRE Implementation	Usage POST Implementation	Percent Change
1	188	425	126.1%
2	193	487	152.3%
3	238	416	74.8%
4	255	512	100.8%
5	257	436	69.6%
6	183	472	157.9%
7	171	452	164.3%
8	156	359	130.1%
9	96	367	282.3%
10	123	523	325.2%
11	281	356	26.7%

Conclusions: A structured, workflow-based dictionary resulted in a large and sustained increase in AE reporting. This overall process improvement can potentially enhance the recognition of defects that may impact patient safety and error reduction in the pathology laboratory.

2033 Influence of External Factors on Frozen Section Performance

JA Wisell, SB Sams. University of Colorado School of Medicine, Aurora, CO.
Background: Pathologists spend their days making decisions, mostly about the significance of histologic features observed during the routine practice of microscopic examination. Recently some have proposed that humans may have an individual capacity for decision-making throughout the day and once exhausted, the quality of this capacity degrades. Here we investigate whether external factors, as suggested by the concept of 'decision fatigue,' may impact upon the ability of a pathologist to render the best possible diagnosis at the time of frozen section (FS).
Design: We evaluated all FS performed within a six-month period at our tertiary level hospital and cancer center. For each FS several features were recorded including the time of day, if the FS diagnosis was discrepant from the final diagnosis and if the diagnosis was deferred at the time of FS. The discrepancies and deferrals were compared to the time of day that they occurred.
Results: Discrepancies and deferrals show a non-uniform frequency throughout the day, which demonstrate a similar pattern of occurrence, showing two periods of increased frequency.

Time	FS volume	Discrepancy (%)	Deferral (%)	Discrepancy or Deferral (%)
<8	112	0	0	0
8-9	178	3.6	0	3.5
9-10	152	3.9	2.2	6.1
10-11	131	7.9	1.3	9.2
11-12	110	3.1	4.6	7.6
12-13	92	2.7	1.0	3.6
13-14	89	3.3	1.1	4.3
14-15	78	4.5	2.2	6.7
15-16	43	7.7	5.1	12.8
16-17	34	4.7	4.7	9.3
17-18	16	8.8	3.9	11.8

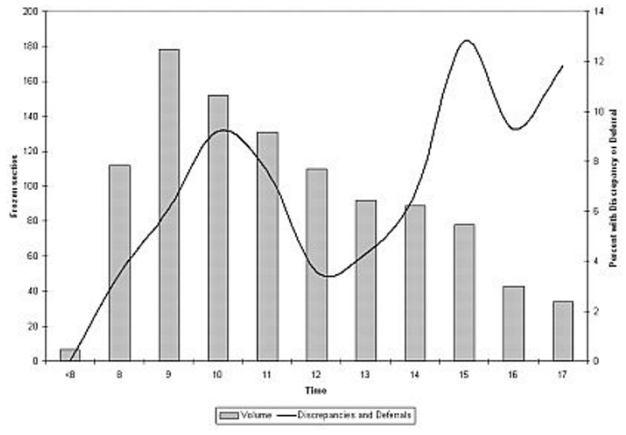

Conclusions: The first period with an increased frequency of discrepancies and deferrals occurs between 10 and 11 am, which follows the busiest period that occurs during the preceding hour. The second period of increased frequency is at the end of the day. The concept of decision fatigue could provide an explanation for this pattern, with increasing discrepancies and deferrals following the morning period of frequent decision-making and again after a full day of decisions. We acknowledge that this may not be the only explanation for our observed pattern of frozen section performance and further investigation will provide additional insight into the factors that underlie these findings. More importantly, further elucidation of influential external factors may provide opportunities for performance improvement initiatives.

2034 Is It Helpful to Further Sub-Classify Thyroid FNA Specimens Diagnosed as Atypia of Undetermined Significance/Follicular Lesion of Undetermined Significance? An Institutional Experience

LQ Wong, VA LiVolsi, ZW Baloch. Hospital of the University of Pennsylvania, Philadelphia, PA.
Background: The overall malignancy rate for the thyroid fine-needle aspiration (FNA) diagnosed as atypia of undetermined significance/follicular lesion of undetermined significance (AUS/FLUS) ranges from 5-30%. It has been recommended to sub-classify AUS/FLUS diagnosis for better patient triage (repeat FNA vs. surgical excision). At our institution, all AUS/FLUS cases include a note regarding the cytomorphologic findings and suspicion for or against a neoplastic process. In this study, we present our experience with cases diagnosed as AUS/FLUS with sub-classifiers.
Design: A search of our laboratory information system was performed to identify all in-house thyroid FNA cases diagnosed as AUS/FLUS from 2008-2011. The data was collected and characterized by patient demographic information, cytopathology diagnosis with sub-classifiers and follow up.
Results: The case cohort included 348 cases diagnosed as AUS/FLUS in 87 males and 261 females. These were sub-classified into one of the following subcategories (SC): SC1 - favor benign, however, a follicular neoplasm (FN) could not be excluded due to increased cellularity; SC2 - specimens with focal nuclear overlapping and crowding; SC3 - scant specimens with focal nuclear overlapping and crowding; SC4 - specimens with focal nuclear overlapping and crowding in a background of lymphocytic thyroiditis; SC5 - few cells with features suspicious for papillary thyroid cancer (PTC), SC6 - specimens in which a FN cannot be excluded (with miscellaneous morphologic descriptors). Of the 348 cases, 13 (4%) were sub-classified as SC1, 127 (36%) as SC2, 128 (37%) as SC3, 52 (15%) as SC4, 17 (5%) as SC5 and 11 (3%) as SC6. Histologic follow-up was available in 139 (40%) cases; 45 (32%) cases were found to be malignant. The malignancy rate for each subcategory was: SC1 - 0%, SC2 - 36%, SC3 - 33%, SC4 - 22%, SC5 - 7% and SC6 - 2%.
Conclusions: Sub-classifying AUS/FLUS diagnosis may prove to be helpful in the management of patients with thyroid nodules.

Techniques

2035 Performance Evaluation Comparison of Three Commercially Available PCR-Based KRAS Mutation Testing Platforms

JA Adams, KM Post, SA Bilbo, X Wang, JD Sen, AJ Cornwell, AJ Malek, L Cheng. Indiana University School of Medicine, Indianapolis, IN.
Background: The identification of KRAS mutations in patients with certain types of cancer, including colonic adenocarcinoma and non-small cell lung carcinoma has become increasingly important as these patients are contraindicated from receiving EGFR-targeted therapies. Several PCR-based tests are commercially available for KRAS mutation testing including Applied Biosystems KRAS Mutation Analysis on the ABI 3130xl, Qiagen therascreen KRAS RGQ PCR on the Rotor-Gene Q MDx and Qiagen KRAS Pyro on the PyroMark Q24, however these tests have not been compared side by side. The purpose of this study was to evaluate the performance characteristics and workflow for three PCR-based methods of detecting KRAS mutation status.
Design: We performed three of the commercially available PCR-based techniques for detecting the KRAS mutation, Applied Biosystems KRAS Mutation Analysis on the ABI 3130xl, Qiagen therascreen KRAS RGQ PCR on the Rotor-Gene Q MDx and Qiagen KRAS Pyro on the PyroMark Q24, on 188 patient samples and Acrometrix standards. The patient samples were of varying tissue types including colorectal, pancreatic, lung, omentum, and diaphragm. The results of each test for every specimen were documented and the three techniques were evaluated for sensitivity, specificity, positive predictive value, negative predictive value, accuracy, workflow, and cost.
Results: All of the 188 samples run were successful, with 29% being positive for the KRAS mutation. Of the positive tests, Applied Biosystems detected 84% of the positive cases, whereas Therascreen RGQ and Pyro detected 100% of the positive cases. In cases of discrepancy between Applied Biosystems and Therascreen RGQ, Pyro agreed with Therascreen RGQ 95% of the time. Therascreen RGQ and Pyro, were comparable in terms of sensitivity, specificity, positive predictive value, negative predictive value, and accuracy, with all values being 100%. All three techniques accurately identified the appropriate mutation in the known control specimens.
Conclusions: All three tests are relatively comparable for detecting the KRAS mutation, with Applied Biosystems having a slightly lower sensitivity, negative predictive value, and accuracy than Therascreen RGQ and Pyro.

2036 Unexpected PAX8 Reactivity in Metastatic High Grade Breast Cancer

KH Adamson, KH Allison, PE Swanson, SM Dintzis, MH Rendi. University of Washington, Seattle, WA.
Background: Metastatic ovarian serous carcinoma and high grade breast carcinoma can be challenging to separate on histologic grounds and treatment options for these neoplasms can vary widely. PAX8 is a lineage-restricted transcription factor that is expressed in genitourinary, thyroid and Mullerian tract epithelial neoplasms, and PAX8 immunohistochemistry (IHC) is often used to differentiate between metastases from high grade breast carcinoma and ovarian serous carcinoma. Previous studies have shown that primary breast carcinomas do not express PAX8 regardless of histologic grade, but data regarding PAX8 expression in metastatic breast carcinoma are limited.
Design: We evaluated 44 Nottingham grade 3 of 3 breast carcinomas (22 primary lesions and 22 metastatic lesions) for expression of PAX8 by IHC using a rabbit polyclonal antibody (Cell Marque; 1:50) and a polymer-based detection system. All

cases were reviewed independently by 2 dedicated breast/gynecologic pathologists. The IHC evaluation included percentage of positive cells and nuclear stain intensity (faint, moderate or strong).

Results: As expected, all primary breast carcinomas were negative for PAX8 (0/22). However, 5 of 22 (23%) metastatic breast carcinomas were PAX8 positive. The fraction of positive cells ranged from <5-30%; stain intensity varied within and between cases:

PAX8 Staining in Metastatic High Grade Breast Cancer

Case	% Positive Cells	Stain Intensity
1	30	Faint
2	<10	Faint
3	<5	Moderate
4	10	Moderate
5	15	Moderate-Strong

Conclusions: PAX8 may be detected in a subset of high grade metastatic breast carcinomas but is generally expressed in a minority of cells. As a result, care should be taken not to over-interpret focal, non-uniform PAX8 expression as indicative of definite ovarian origin in high grade metastatic carcinomas.

2037 Comparison of Three BRAF Mutation Tests in Formalin-Fixed Paraffin Embedded Clinical Samples

S Ahn, J Lee, J-Y Sung, SY Kang, K-M Kim. Samsung Medical Center, Sungkyunkwan University School of Medicine, Seoul, Republic of Korea; School of Medicine, Kyung Hee University, Seoul, Republic of Korea.

Background: Recently, BRAF inhibitors showed dramatic treatment outcome in BRAF V600 mutant melanoma. Therefore, the accuracy of BRAF mutation test is critical for proper patient selection who are indicated for BRAF inhibitors.

Design: A total of 64 tumors including 34 malignant melanomas, 16 papillary thyroid carcinomas, and 14 carcinomas from other primary sites were analyzed for BRAF mutation. BRAF mutations were detected by allele-specific PCR (AS-PCR) and direct sequencing and subsequently retested with a real-time PCR assay, cobas 4800 V600 mutation test. The results of cobas were directly compared to those of AS-PCR and direct sequencing.

Results: There was 90.6% concordance (58 of 64 tested samples) and 9.4% discordance among the 3 methods. Out of 6 discordant cases, 4 cases were melanomas and two cases were papillary thyroid carcinomas. Three cases were BRAF V600E positive only by cobas test, but were not detected by AS-PCR and direct sequencing. One melanoma patient with BRAF detected only by cobas test, but wild in both AS-PCR and direct sequencing has been on vemurafenib treatment for 6 months and showed a dramatic response to vemurafenib. AS-PCR failed to detect a V600K mutation in a case which was identified by direct sequencing and cobas test.

Conclusions: In conclusion, we directly compared cobas test with currently available AS-PCR and direct sequencing for BRAF mutation and found that cobas test is a reliable method to be applicable in small quantities of DNAs extracted from FFPE clinical samples.

2038 Image-Guided Coring for Large-Scale Projects in Molecular Oncologic Pathology

GM Baker, L Montaser, N Knoblauch, S Christensen, A Hazra, R Tamimi, LC Collins, AH Beck. Beth Israel Deaconess Medical Center & Harvard Medical School, Boston, MA; Brigham and Women's Hospital, Harvard Medical School, Boston, MA.

Background: Recent advances in molecular pathology permit a wide range of DNA- and RNA-based assays to be performed on archival formalin-fixed paraffin-embedded tissue (FFPE). Three commonly used techniques are laser-capture microdissection (LCM), macro-dissection from unstained slides, and direct coring of a block via a needle. While precise, LCM is extremely labor intensive making it impractical for most large-scale projects. Also labor intensive, macro-dissection requires manually scraping tissue from multiple slides per case. Although coring is by far the least labor intensive method, it is also potentially the least accurate and most error-prone method as the standard approach involves manual alignment of an annotated glass slide with an FFPE block followed by the attempt to manually sample designated regions of interest on the FFPE block. This traditional coring approach is especially problematic for small lesions. To overcome these limitations we have implemented an image-guided coring (IGC) procedure for molecular analyses.

Design: Whole slide digital scans of H&E-stained slides are acquired using the Panoramic SCAN (3D-Histech) and a pathologist selects regions of interest from these digital images using the PannoramicViewer Software package (3D-Histech). This annotated image is overlaid onto a digital image of the FFPE block using TMA-Master software (3D-Histech) and a computer-guided robotic arm is prompted to accurately sample the selected regions of the FFPE block. This selectively acquired tissue can then be used in downstream molecular analyses.

Results: IGC was performed on 300 breast cancer cases from the Nurses' Health Study with subsequent RNA extraction from both invasive cancer and normal terminal duct lobular units for downstream molecular analysis. A high success rate of adequate RNA (ng/mL) extraction from tumor and normal tissue via IGC has been obtained (88% and 64.79%, respectively).

Conclusions: IGC is an effective new approach for sampling FFPE tissue blocks, thereby serving as a valuable tool to link molecular assays to cancer morphology. Furthermore, IGC provides an ideal balance between precision and efficiency for large-scale projects in molecular oncologic pathology.

2039 Mutational Load Quantification Technique as an Aid to the Histopathologic Evaluation of Barrett's Esophagus

WW Bivin, Jr., S Patel, JF Silverman, B Corcoran, E Ellsworth, S Jackson, S Finkelstein. Allegheny General Hospital, Pittsburgh, PA; RedPath Integrated Pathology, Inc., Pittsburgh, PA.

Background: Histopathologic evaluation of dysplasia in Barrett's esophagus (BE) is often challenging with significant interobserver variation. We developed a quantitative mutational load (ML) scoring system as an aid to define disease progression along the spectrum from intestinal metaplasia, through dysplasia to cancer in BE. We hypothesize that ML quantification scoring technique helps recognize mutation count and clonality in stages of disease progression.

Design: We examined formalin-fixed, paraffin-embedded gastroesophageal junction biopsies and esophageal mucosal resections from 22 patients. From these cases, 32 microdissection targets in intestinal metaplasia (IM, n=4), low grade dysplasia (LGD, n=7), high grade dysplasia (HGD, n=13) and carcinoma (CA, n=8) were made and tested for both loss of heterozygosity and microsatellite instability in a panel of 22 microsatellite markers at 10 loci using PCR/capillary electrophoresis. The proportion of cells affected was quantitatively determined, with high clonality mutations representing >75% of cells, and low clonality representing 50-75%. ML was calculated using numbers of low and high clonality mutations and the number of loci affected by microsatellite instability.

Results: All targets in this series showed mutations and a ML increase was present along the sequence of intestinal metaplasia to dysplasia to carcinoma. Microdissected targets with histologic intestinal metaplasia had MLs in the range of 0.50-2.00 (average 0.94). Targets with LGD had mutational loads slightly higher in the range of 1.00-2.50 (average 2.00). The ML between IM and LGD was not significant (p = 0.42). MLs in targets of HGD ranged from 1.50-6.50 (average 3.77), and targets with carcinoma showed the highest ML (average 5.25). The ML between HGD and CA was not significant (p = 0.043). However, the ML between IM/LGD versus HGD/CA was significant ($p < 0.0001$).

Conclusions: 1.) The technique for evaluating mutational load at individual microdissection targets of BE is quantifiable and can provide useful complementary information for the histopathologic evaluation for dysplasia or malignancy in BE. 2.) ML quantification can be especially helpful in separating LGD from HGD, which can be occasionally challenging in H&E examination.

2040 Validation of Dual Color HER2/Chromosome 17 ISH (In-Situ Hybridization) – Comparison with Single Color CISH (Chromogenic In-Situ Hybridization) and Inter-Observer Reproducibility

MP Branscomb, JR Ross, D Horton, MS Rasco, TS Winokur, VV Reddy, S Wei, S Harada. University of Alabama at Birmingham, Birmingham, AL.

Background: Evaluation of HER2 status is important in breast cancer management. Fluorescent in-situ hybridization (FISH) is considered the standard method, although brightfield in-situ hybridization (ISH) has several advantages including certainty of recognizing tumor cells and stability of the signals. Recently, dual color brightfield ISH has become available. In this study, dual color HER2 ISH testing was compared with HER2 single color CISH testing, currently offering clinically in our institution.

Design: Forty-seven cases with invasive breast carcinoma were selected based on HER2 CISH test (Invitrogen SPOT-LIGHT) results (50 cases were selected originally and 3 cases were excluded due to lack of tumor cells on the section; 22 amplified, 22 non-amplified, and 3 equivocal). Dual color HER2/Chromosome 17 ISH (Ventana INFORM) were performed on these cases. Dual color ISH results were evaluated by four pathologists independently who were blinded to any information and the results were compared with CISH results. For discrepant cases, final calls were made at the QA conference.

Results: All 22 cases called non-amplified by CISH were called non-amplified by Dual color ISH assay and there was no inter-observer variation. Among 22 cases called amplified by CISH, one case was called non-amplified because the areas showing amplification were not present in the section used for Dual color ISH. The remaining 21 cases were called amplified. Two of these cases showed inter-observer variation. Two of three equivocal cases showed inter-observer variation with one called amplified and the other non-amplified. Third case was called non-amplified due to polysomy, which cannot be evaluated by CISH.

Table 1: Concordance between single color CISH and Dual color ISH

	Single Color CISH		
Dual Color ISH	Amplified	Equivocal	Non-Amplified
Amplified	21	1	0
Non-Amplified	1*	2	22

* The areas showing amplification in CISH were not present in the section used for Dual color ISH

Overall, concordance rate between two assays was 97.7%. Inter-observer concordance rate was 91.5% with Cohen's kappa 0.907. Four cases showing inter-observer variation appear to have tumor heterogeneity.

Conclusions: In conclusion, Dual-color HER2/Chromosome 17 ISH assay showed an excellent performance with added advantage of ability to distinguish true amplified cases from polysomy without amplification. This assay may be a better alternative to the currently most commonly used FISH assay.

2041 Colorimetric Detection of Prostate Cancer in Grid Regions Utilizing a Ratio of Racemase to High Molecular Weight Keratin (HMWK) and P63

BM Brasseur, AD Johnson, JC Henrikson, JS Koopmeiners, KB Daniels, GJ Metzger, SC Schmechel. University of Minnesota, Minneapolis, MN.

Background: For prostate cancer(Pca) laboratory studies, correlating preoperative prostate magnetic resonance(MR) spectroscopy features with postoperative

reconstructed whole organs(from pathology slides) and quantifying relative proportions of carcinoma, benign epithelium, stroma and gland spaces would allow weighting of each tissue component during statistical analysis. We developed SigMap software that aligns pathology whole slide images(WSI) and generates grid regions in which tiled protein expression data using immunohistochemistry(IHC) may be generated across tissues(PMID:22438942). We are investigating whether IHC stains for racemase and basal cell markers may facilitate quantifying relative amounts of carcinoma(racemase developed with Fast Red chromagen), benign epithelium(p63 and HMWK basal cell markers developed with diaminobenzidine), stroma(blue hematoxylin counterstain) and gland lumens(white) areas within grid regions.

Design: Ten PCa-containing blocks were randomly selected. One section was stained with H&E; an adjacent section was stained with racemase, HMWK, and p63(and hematoxylin counterstain) using an automated platform(Ventana). Slides were digitized(ScanScope XT, Aperio) and PCa areas were annotated by pathologists. SigMap software aligned the sections and generated virtual 0.5 x 0.5 mm grid squares across tissues; color deconvolution(Aperio) software was used to quantify IHC stains. Fractional percentages of red, brown, blue and white, as well as red:brown ratios were calculated.

Results: Of an average 1080 total grid regions per slide, on average 27% of the regions contained PCa(range=0.9-54%). Red-stained pixels comprised a higher percentage of PCa-annotated grids(23.5%, SD= 14.6) than in non-PCa grids(2.75%, SD=0.91, p=0.0015). Brown-stained pixels comprised a lower percentage in PCa grids(2.18%, SD=1.29) vs non-PCa grids(4.84%, SD=1.58%, p=0.00069). The average red:brown ratio was 21.6-fold higher in PCa grids vs non-PCa grids(p= 0.0002). There was less blue-stained area in PCa grids(57.4%, SD=13.2) vs non-PCa grids(68.2%, SD=2.6, p=0.031), indicating a higher proportion of stroma in benign areas. There was less white area(16.9%, SD=6.1) in PCa grids vs non-PCa grids(24.2%, SD=2.1, p=0.0042), indicating a higher proportion of luminal area in benign tissue.

Conclusions: Racemase and basal cell IHC stains within computer-generated grid regions may be useful to determine the fractional composition of carcinoma, benign epithelium, stroma, and gland lumens. Also, a ratio of racemase:basal cell markers may be useful in automatically annotating PCa.

2042 Utility of *MLH1* Methylation Analysis in the Clinical Evaluation of Lynch Syndrome in Women with Endometrial Cancer

A Bruegl, B Djordjevic, D Urbauer, R Luthra, R Broaddus. MD Anderson Cancer Center, Houston, TX; Ottawa Hospital, University of Ottawa, Ottawa, ON, Canada.

Background: Immunohistochemistry and microsatellite instability are important screening tools to evaluate endometrial cancer (EC) patients for Lynch Syndrome. A complicating factor is that 15-20% of sporadic EC have immunohistochemical loss of MLH1 and high levels of microsatellite instability due to methylation of *MLH1*. The PCR-based *MLH1* methylation assay resolves this issue, yet many clinical laboratories do not perform this assay. The objective of this study was to determine if clinical or pathologic features help to distinguish sporadic EC with MLH1 loss secondary to *MLH1* methylation from Lynch Syndrome-associated EC with MLH1 loss and absence of *MLH1* methylation.

Design: For 337 EC, MLH1 immunohistochemistry and PCR-based *MLH1* analysis were performed. Clinical and pathological data were collected for all patients.

Results: 54/337 EC (16%) had immunohistochemical loss of MLH1. 40/54 had *MLH1* methylation and were designated as sporadic, while 14/54 lacked *MLH1* methylation and were designated as probable Lynch Syndrome. Diabetes and deep myometrial invasion were significantly associated with the probable Lynch Syndrome group; no other clinical or pathological variable distinguished the 2 groups. Combining Society of Gynecologic Oncology screening criteria with these 2 features accurately captured all Lynch Syndrome cases, but with very low specificity of 36%.

Endometrial Carcinomas with Immunohistochemical Loss of MLH1

	Sporadic - Methylated MLH1 (%)	Probable Lynch Syndrome - Unmethylated MLH1 (%)	p-value
Median Age (range)	57 (31-92)	52 (42-79)	0.4295
Median BMI	32.9	30.9	1.0
Family History Endometrial Cancer	4 (10.5)	3 (21.4)	0.370
Family History Colon Cancer	7 (18.4)	3 (21.4)	1.0
Diabetes	4 (10)	6 (42.9)	0.013
Endometrioid Histology	35 (87.5)	11 (78.6)	0.413
FIGO Stage I or II	27 (67.5)	11 (78.6)	0.515
Endometrioid Grade 1 or 2	26 (74.3)	9 (81.8)	1.0
Deep Myometrial Invasion	15 (37.5)	10 (71.4)	0.035
LVSI	24 (60.0)	8 (57.1)	1.0
Lower Uterine Segment Tumor Location	3 (7.5)	3 (21.4)	0.173
Tumor Size Less Than 4 cm	21 (52.5)	8 (57.1)	1.0

Conclusions: No single clinical/pathologic feature or screening criteria tool accurately identified all Lynch Syndrome-associated endometrial carcinomas with acceptable specificity. The *MLH1* methylation assay should thus be included in the clinical work-up of these patients.

2043 Use of Locked Nucleic Acid Probes (LNA) Greatly Increases Sensitivity of Sanger Sequencing (SS): A Comparative Experience of Genotyping of KRAS Codons 12,13

DA Chitale, L Whiteley, L Szymanski, M Cankovic. Henry Ford Hospital, Detroit, MI.

Background: Targeted therapies in pursuit of personalized medicine are growing in number due to new biomarker discoveries. Emerging treatment protocols are using this approach as first-line therapies and the companion diagnostic tests are being ordered on smaller biopsy samples. This has raised the challenge on the molecular laboratories to provide rapid, reliable, accurate and sensitive methods for mutation screening of very limited samples. SS of PCR-amplified DNA, the most widely used method, has limitation due to low sensitivity (~[/underline]20-25%). Our aim was to improve the performance of lab developed SS based KRAS mutation assay by modified Sanger sequencing (MSS) with LNA and compare it with allele specific PCR (AS-PCR) and use this as a pilot project to expand on other SS based assays.

Design: To increase the sensitivity of routine SS, we modified the standard PCR assay by adding LNA probes to favor mutant DNA amplification during PCR. Mutations in KRAS codon 12, 13 using SS and MSS were evaluated. Samples were also run on Qiagen's KRAS RGQ PCR kit to detect 7 somatic mutations using real time PCR and using Scorpions and ARMS® technologies (AS-PCR). 21 clinical samples [9 primary adenocarcinomas (7 colorectal,2 lung) and 12-metastatic colorectal adenocarcinomas at various sites] and a dilution series of known positive KRAS mutant cell line were tested in parallel using the 3 above methods. All samples were either formalin-fixed, paraffin-embedded tissues or cytology slides. Manual macrodissection was performed when tumor cellularity was less than 50% of total cells(10/21 cases).

Results: MSS-LNA method detected 3 additional mutations compared to SS and 1 additional mutation compared to AS-PCR. Sensitivity of the assay was determined to be 1% by MSS-LNA & Qiagen KRAS RGQ PCR kit & 20% for SS.

Type of tissue	# of cases 21	Sanger sequencing	Modified sanger sequencing-LNA	AS-PCR	Concordant vs Discordant
Abdominal wall, metastasis	1	+	+	+	C
Bladder, metastasis	1	-	-	-	C
Colon, primary	5	-	-	-	C
		-	-	-	C
		-	-	-	C
		+	+	+	C
		+	+	+	C
Liver, metastasis	2	+	+	+	C
		-	+	-	D
Lymph node, metastasis	3	+	+	+	C
		-	+	+	D
		+	+	+	C
Lung- 2 primary, 2 metastasis (one cytology smear-primary)	4	+	+	+	C
		+	+	+	C
		+	+	+	C
		-	+	+	D
Omentum, metastasis	1	+	+	+	C
Ovary, metastasis	2	-	-	-	C
		-	-	-	C
Rectum, primary	2	+	+	+	C
		-	-	-	C

Conclusions: MSS-LNA method increased the detection sensitivity of SS 20-fold, equivalent or more sensitive than AS-PCR. This is not only a cost effective method, but also offers wider coverage for discovering additional rarer mutations not detected by AS-PCR. MSS-LNA method needs much less DNA and thus is a reliable and sensitive method for detecting mutations in any sample type, especially where the sample size is limited or paucicellular.

2044 Out of the Dark into the Light: Brightfield Dual In Situ Hybridization as a Modality for Assessing HER2 Gene Amplification in Invasive Urothelial Carcinoma

P Cotzia, A Bombonati, R O'Neill, D Jaller, R Draganova-Tacheva, C Solomides, S Peiper, P McCue, R Birbe. Thomas Jefferson University Hospital, Philadelphia, PA.

Background: HER2 gene amplification has been reported as a survival predictor in muscle-invasive urothelial carcinoma (UCa). The current modality for assessing the HER2 positivity is the one used in breast cancer. It follows a two step process with HER2 immunohistochemical stain (IHC) and confirmatory fluorescent in situ hybridization (FISH). Tumor heterogeneity and polysomy 17, commonly found on UCa, limits the usefulness of these techniques. FISH requires a fluorescence microscope and the signal attenuates with time. More than "working in the dark", FISH forces the pathologist to work in the dark on a histologic level as well. Brightfield HER2 dual color in situ hybridization (HER2 Dual ISH) ameliorates these limitations, is permanent, storable, and less technically demanding. It enables the diagnosis of HER2 amplification and polysomy 17 in the context of morphology.

Design: After IRB approval, we searched retrospectively invasive UCa (resection and cystectomy) and benign controls. Seventy invasive high grade UCa and 5 benign bladders were selected. The diagnosis was confirmed with the H&E slides. A 2 mm tissue core microarray was performed from the formalin fixed-paraffin embedded tissue blocks using the Veridiam tissue arrayer. HER2/neu IHC and HER2 Dual ISH tests were performed using the anti-HER2/neu (4B5) rabbit monoclonal primary antibody and the INFORM HER2 Dual ISH DNA Probe Cocktail according to the manufacturer's protocols (Ventana Medical Systems). The results were analyzed by three pathologists following the breast cancer guidelines. A chromosome (Chr) 17 average above 2.2 signals per 20 cells was diagnosed as polysomy 17 on the HER2 Dual ISH test.

Results: HER2 gene was amplified in 4 of 70 (5.7%) invasive UCa but not on the 5 benign bladders (0%). HER2 was overexpressed (3+) in 18 UCa cases (25.7%); including all 4 amplified cases. 77.7% of the HER2 3+ cases were not amplified. 26 UCa cases had HER2 2+ indeterminate results (37%), none of them were amplified; however 20 of 26 (76%) had polysomy 17. Polysomy 17 was present on 55 of the 70 UCa cases (78%) including 3 of the HER2 Dual ISH amplified cases.

Conclusions: HER2 overexpression and Dual ISH amplification have 100% concordance in UCa. Commonly HER2 overexpression is due to polysomy 17 rather than HER2 gene amplification limiting the value of HER2 IHC testing. HER2 Dual ISH might be a superior single test to detect HER2 gene amplification than the classic two-step process IHC and FISH in invasive UCa.

2045 Concordance Study Reveals a Higher Performance of OSNA over Morphologic Techniques To Detect Lymph Node Metastasis in Papillary Carcinoma of the Thyroid

S del Carmen, S Gatius, C Garcia-Macias, JA Baena-Fustegueras, G Franch-Arcas, P Galindo, A Perez, J Pallares, D Cuevas, X Matias-Guiu, E de Alava. Salamanca University Hospital-CIC-IBSAL, Salamanca, Spain; Arnau de Vilanova Hospital, Lleida, Spain.

Background: Surgical treatment of papillary thyroid carcinoma (PTC) includes central compartment (CC) lymphadenectomy. This is positive in about one third of cases. Sentinel node biopsy of CC has a high positive predictive value. However, conventional intraoperative diagnostic assays have a 17% rate of false negatives. Lymph node (LN) analysis by means of One-Step Nucleic Acid Amplification (OSNA) assay is a procedure used for intraoperative staging of breast cancer patients, based on real-time amplification & quantitation of CK19 mRNA in LN samples. Since CK19 is also expressed in PTC, our aim is to determine utility of OSNA for intraoperative detection of LN metastasis of PTC in comparison with conventional morphologic intraoperative assays (cytology imprints (CYT) and H&E stain on completely serially sectioned (CSS) paraffin-embedded LN.

Design: We studied 186 consecutive LN in 17 patients with diagnosis of PTC. Each LN was weighted and bisected. One LN half was entirely submitted for OSNA. The other one was paraffin-embedded and CSS (which we considered as the gold standard). Two CYT were taken from each LN half and stained for H&E and CK19. We assessed: i) Concordance between CYT from both LN sides (H&E and CK19). ii) Concordance between CYT and CSS. iii) Sensitivity of OSNA and CYT with respect to CSS.

Results: i) 240 CYT from both sides were available for H&E staining; concordance was seen in all but 5 cases (97.9%). 238 pairs of CYT from both sides were available for CK19 staining; concordance was seen in all but 6 cases (97.4%).

ii) CCS was available in 49 cases. Concordance between CSS results and CYT results was seen in 45 cases (91.8%). In two cases, CSS was positive and CYT was negative. In another two cases CSS was negative and CYT was positive.

iii) Comparison between OSNA results and CYT could be performed in 180 LN. Concordant results were obtained in 156 LN (86.7%). In 16 LN (8.9%), positive OSNA results were obtained together with negative CYT. Negative OSNA results and positive CYT were obtained in 8 LN (4.4%); in 3 of them a low copy number of CK19 mRNA was seen, suggesting that the cutoff value for OSNA results in PTC could be lowered. Overall sensitivity of OSNA was 78.5%, above that of CYT (64.2%).

Conclusions: OSNA assay is feasible for intraoperative detection of lymph node metastasis of PTC. Its sensitivity is significatively higher than that of conventional intraoperative assays. Performance of CYT is in our hands similar to that of CSS to detect PTC.

2046 Use of Digital Slide Imaging for the Establishment of a Quantitative Database of Meningioma Cellularity

C Dowlatshahi, R Emmadi, K Brinyiczki, T Valyi-Nagy. University of Ilinois Hospital and Health Sciences System, Chicago, IL.

Background: The grading of meningiomas includes some subjective criteria such as the determination of the presence or absence of increased cellularity. No firm objective and quantitative criteria have been established to guide pathologists in this task. The objective of this study is to establish a quantitative database of meningioma cellularity that can be used as a reference for more objective meningioma grading.

Design: To establish a quantitative database of meningioma cellularity, 205 meningiomas diagnosed at our Institution between January 2006 and August 2012 were identified for this study. Cases included 137 WHO grade I, 66 WHO grade II, and 2 WHO grade III meningiomas. Hematoxylin and eosin-stained sections of all cases are scanned using a Hamamatsu Nanozoomer 2.0 HT digital slide scanner. Digitalized whole slide images are reviewed by two independent observers and two 0.16 square millimeter areas of each tumor demonstrating the highest cellularity are selected and assessed for the number of meningioma cells by manual counting. Tumor cell counts generated by the independent observers are included into the determination of the cellularity of each case and based on these measurements, the mean, median, range and standard deviation of the cellularity of the studied reference meningioma set will be determined.

Results: Ten meningiomas have so far been assessed for cellularity in this ongoing study. Observations collected so far indicate mean and median meningioma cellularity of 964 and 968 tumor cells per 0.16 square millimeters, respectively, with a standard deviation (SD) of means of 193 and a range of 689 to 1253 (n=10). The measurements for different grades of meningioma were: (i) for WHO grade I meningiomas (n=5): mean= 837, SD of means=130, median=780, range= 689 to 993; and (ii) for WHO grade II meningiomas (n=4): mean= 1077, SD of means=176, median=1097, range=862 to 1253. Cellularity of the single case of WHO grade III meningioma analyzed so far was 1143 per 0.16 square millimeters.

Conclusions: Our initial observations indicate that determination of meningioma cellularity is feasible with the use of digital slide imaging. When completed, this study will establish a quantitative database of meningioma cellularity that will be a useful and practical reference tool for a more objective meningioma grading.

2047 Ki67 Evaluation in Breast Cancer: Molecular Pathology Using Digital Imaging

K Drak Alsibai, S Azoulay, O Languille-Mimoune, B Poulet, A Barres, C Adem. Institut de Pathologie de Paris, Paris, France.

Background: Proliferation is of major interest in breast cancer management. Ki67 evaluation is considered as a strong surrogate marker for classifying tumors. It is widely available and its evaluation done by routine light microscopy. Proliferation markers are also included in the approved molecular chips dedicated to breast cancer. Our objective was to compare the evaluation of Ki67 by routine microscopy, with its evaluation by digital imaging using different methods (whole slide versus hotspot).

Design: Breast cancer cases were prospectively collected over a time period. Pathologists reported Ki 67 score as they did routinely according to the current recommendation (Dowsett M, JNCI 2011). After their report signed out, all slides were scanned using Ventana iScan Coreo. Digital slides were evaluated by the mean of Virtuoso (software, Ventana Roche). Two digital measurements were made, appreciation of the hostpots and then the whole slide (as if it was macrodissected for molecular technique). All values were compared and discrepancies noted.

Results: Complete date was available for 48 cases (19 biopsies, 29 surgical specimens). Since there is no consensus on the threshold for Ki67 to classify highly proliferating tumor versus low proliferating tumor, three different analyses were conducted across all three methods (routine, hotspot, whole slide); using 14% cutoff showed 14 discordant cases (29%), while using either 20% or 30% cutoff showed 6 discordant cases (14%). Comparing hotspot versus whole slide evaluation showed higher mean index for the former (20%) compared to the latter one (14%), as expected because of the stromal cells included in the whole slide analysis. Again in this latest comparison, either 20% or 30% cutoff showed only 4% discordant cases while 21% discordant cases were seen if the cutoff was set at 14%.

Conclusions: Digital imaging of whole slide might increase robustness of Ki67 evaluation in comparison with molecular high throughput technologies. As for Her2 score 2, Ki67 evaluation could have an equivocal index range, such as 1 to 30%, where further evaluation (independent interpretation by another pathologist or digital imaging) should be recommended. Combining biomarkers and standardized evaluation by immunohistochemistry in a complex mathematical algorithm (such as IHC4) could therefore help in a better management of a specific subset of breast cancer patients.

2048 Digital Imaging in Breast Cancer: An Ode to Microscopy

K Drak Alsibai, S Azoulay, O Languille-Mimoune, B Poulet, A Barres, C Adem. Institut de Pathologie de Paris, Paris, France.

Background: Digital image analysis is currently available using strong electronic algorithm in order to evaluate biomarkers (ER, PR, Her2 and Ki67) in breast pathology. Our objective was to compare this technology with the routine manual appreciation of the mentioned breast biomarkers.

Design: Breast cancer cases were prospectively collected over a time period. Pathologists reported breast panel as they did routinely according to the ASCO/CAP recommendation. After their report signed out, all slides were scanned using Ventana iScan Coreo. Digital slides were evaluated by the mean of Virtuoso (software, Ventana Roche). All values were compared and discrepancies noted.

Results: Complete date was available for 59 cases (23 biopsies, 36 surgical specimens). There was no discordant result in ER evaluation (8 ER-; 51 ER+) using both methods. Six cases (10%) were scored differently for PR (three considered negative or positive by either method). Digital evaluation for Her2 reported more score 3 than manual scoring (12 cases versus 9; 20% versus 15%), more score 2 (17% versus 12%), but less scores 0/1 (63% versus 73%). Interestingly, SISH was available and showed gene amplification for 2 discordant cases reported manually score 2, and by image analysis score 3. No Her2 amplification was seen by SISH in another case scored 2 by both methods. Since there is no consensus on the threshold for Ki67 classifying highly proliferative tumor versus low proliferative tumor, three different analyses were done: using 14% cutoff showed 11 discordant cases, while using 20% cutoff showed 8 discordant cases, and 30% cutoff showing 3 discordant cases (5%).

Conclusions: Manual evaluation of breast cancer biomarkers remains the gold standard as it can be used by all pathologists. It is a cost effective method, as well as time saving. Digital imaging may help in training pathologists, or when applied on low proliferative tumor. Recommendations from consensus conference might emphasize using different approaches: routine microscopy as 1st screening, and in some instances depending on the final advocated cutoff either independent reading by two pathologists or the use of digital imaging.

2049 BRAF Mutations in Metastatic Malignant Melanoma: Comparison of Molecular Analysis and Immunohistochemical Expression

L Ehsani, C Cohen, KE Fisher, MT Siddiqui. Emory University Hospital, Atlanta, GA.

Background: Melanoma is a complex genetic disease, and multiple genetic alterations have been reported to play a role during disease progression. The dysregulation of BRAF signaling has been shown to affect many molecules that promote the continual progression of melanoma. Oncogenic BRAF expression plays a vital role in promoting cell invasion and metastasis in melanoma. It is also associated with poor prognosis in metastatic melanoma. 40% to 60% of cutaneous melanomas have BRAF mutations and about 90% of the mutations involve a specific substitution at codon 600 (BRAF

V600E). In this study, we compared BRAF (V600 E) mutation detection by molecular analysis with BRAF expression by immunohistochemistry (IHC).

Design: We selected 25 cases of metastatic malignant melanoma, 19 excisional biopsies and 6 fine needle aspiration cell blocks (CB). BRAF V600 E mutations were detected using the COBAS® 4800 BRAF V600 Real-time PCR assay and IHC expression with the Dako Autostainer, the BRAF V600 EP152Y monoclonal antibody (Abcam, 1:20), and high pH antigen retrieval (Trilogy, Cell Marque). IHC results were interpreted as positive if more than 10% of melanoma cells showed cytoplasmic staining of 2+ or 3+ intensity. Three pancreatic lesions were immunostained as negative controls. Molecular analysis was used as the gold standard for statistical analysis.

Results: 10/25 (40%) cases were positive by molecular analysis and 17/25 (68%) cases by IHC. All positive cases by molecular analysis were positive by IHC (100%). All 3 (100%) negative controls were negative.

Statistical analysis of BRAF V600 mutation by molecular analysis and IHC

	Sensitivity	Specificity	PPV	NPV	Accuracy
IHC	100%	53%	59%	100%	72%

Conclusions: Molecular testing for the BRAF V600 E mutation in metastatic malignant melanoma remains the more accurate and sensitive methodology. IHC yields a very high sensitivity but, due to increased false positivity, the specificity is much lower which may be due to the presence of other BRAF point mutations. However, IHC testing is less expensive and widely available to most laboratories when compared to molecular analysis. Hence, it can be useful for initial screening evaluation of BRAF mutations in metastatic malignant melanoma. Molecular testing can be supplemental for IHC positive or equivocal cases, as a confirmatory test resulting in considerable cost containment.

2050 Immunohistochemistry for Novel Markers in Squamous Cell Carcinoma: Glypican-3 Is Expressed across Anatomic Sites, PAX8 Is Limited in Distribution, and p40 Is Extremely Sensitive

MP Gailey, AM Bellizzi. University of Iowa Hospitals and Clinics, Iowa City, IA.

Background: Immunohistochemistry (IHC) is generally not considered helpful in assigning the site of origin of a squamous cell carcinoma (SCC). TTF-1 and p16 are modestly useful exceptions. In this vein, we were intrigued by a few recent observations: 1. glypican-3 (GPC3), an oncofetal protein often used in hepatocellular carcinoma (HCC) diagnosis, was identified in gene expression profiling of lung tumors and found to be overexpressed in lung SCC; 2. PAX8, a transcription factor critical in thyroid, kidney, and Müllerian tract, was expressed by a few SCC's in large scale IHC studies; 3. p40, an antibody specific for the ΔNp63 isoform, is gaining traction as an SCC marker due to superior specificity in lung. We examined expression of these 3 proteins in SCC's from diverse anatomic sites and in urothelial carcinoma (UC) (histologically similar/often showing squamous differentiation).

Design: IHC for GPC3, PAX8, and p40 was performed on whole sections from 107 SCC and 11 UC. Slides were independently scored (intensity/extent of staining) by 2 pathologists, blinded to site. Granular, cytoplasmic GPC3 staining in ≥5% of tumor cells and any definite PAX8/p40 nuclear staining were considered positive. Discrepancies were resolved over a two-headed microscope.

Results: Overall, GPC3 was seen in 22/118 (19%) tumors (9 of 12 sites), PAX8 was restricted to cervix and bladder, and p40 was seen in all but 1 tumor (minute focus of residual tumor in a treated esophagus). PAX8 and p40 slides were scored with 100% and GPC3 slides with 93% concordance. Site specific results are shown in the Table.

Protein Expression by Anatomic Site

	GPC3 (n, %)	PAX8 (n, %)	p40 (n, %)
Anus	1/10 (10%)	0/10 (0%)	10/10 (100%)
Bladder (UC)	1/11 (9%)	2/11 (18%)	11/11 (100%)
Cervix	3/11 (27%)	3/11 (27%)	11/11 (100%)
Esophagus	2/7 (29%)	0/7 (0%)	6/7 (86%)
Larynx	3/10 (30%)	0/10 (0%)	10/10 (100%)
Lung	6/12 (50%)	0/12 (0%)	12/12 (100%)
Penis	0/10 (0%)	0/10 (0%)	10/10 (100%)
Skin	0/10 (0%)	0/10 (0%)	10/10 (100%)
Ventral Tongue/Floor of Mouth	1/8 (13%)	0/8 (0%)	8/8 (100%)
Tongue Base/Tonsil	1/8 (13%)	0/8 (0%)	8/8 (100%)
Vagina	4/10 (40%)	0/10 (0%)	10/10 (100%)
Vulva	0/11 (0%)	0/11 (0%)	11/11 (100%)

Conclusions: GPC3 is not specific to lung SCC and, instead, is often expressed across anatomic sites; pathologists are cautioned against over-relying on this marker in making a diagnosis of HCC. PAX8 is limited in distribution and may have a use in assigning site of origin. p40 is extremely sensitive for SCC (and UC); further studies evaluating its specificity at other sites (e.g., GI/GYN tracts) are warranted.

2051 The Ventana INFORM HER2 Dual In Situ Hybridization (DISH) DNA Probe Cocktail Assay Versus Fluorescence In Situ Hybridization (FISH): Focussed Study of Immunohistochemical 2+ Cases

FF Gao, DJ Dabbs, R Bhargava. Magee-Womens Hospital of University of Pittsburgh Medical Center, Pittsburgh, PA.

Background: The Ventana INFORM HER2 Dual in-situ hybridization (DISH) DNA probe cocktail assay is a new FDA approved technique designed to determine HER2 gene status by using light microscopy. We compared this new methodology with standard fluorescence in situ hybridization (FISH) on the most challenging group of breast cancers, i.e. HER2 immunohistochemical (IHC) 2+ cases.

Design: This prospective validation study was performed on 104 invasive breast cancer cases with equivocal HER2 IHC results (IHC score 2+). Both FISH and DISH were performed on the same tumor blocks. The DISH assay staining results were enumerated by counting at least 20 nuclei by an experienced pathologist blinded to FISH results. Similar to FISH, areas with stronger IHC staining were counted in heterogeneous cases. For both FISH and DISH, HER2 amplification was defined as HER2/Chr17 ratio 2.0. Cases with HER2/Chr17 ratio <2.0 were considered as non-amplified. In addition, 20 HER2 IHC 3+ invasive carcinoma cases (represented on a tissue microarray) were also evaluated by DISH.

Results: DISH was successful in 96 of 104 cases (92%) in the first attempt. Of the 8 cases that failed the first time, 7 cases showed optimal signals on repeat DISH, with overall success rate of 99% with 2 attempts. The overall concordance between FISH and DISH was 92% for these IHC 2+ cases (see table). Four cases were amplified by FISH and not amplified by DISH. The HER2 to Chr17 ratio on these 4 cases by FISH ranged from 2.04 to 2.06. Four cases were amplified by DISH and not amplified by FISH. The HER2 to Chr17 ratio on these 4 cases by DISH ranged from 2.08 to 2.58. All 20 (100%) IHC 3+ cases showed clusters of HER2 gene consistent with HER2 amplification by DISH.

	DISH Amplified	DISH Not Amplified	Total
FISH Amplified	7	4	11
FISH Not Amplified	4	88	92
Total	11	92	103

1 case failed by DISH in 2 attempts.

Conclusions: The Ventana INFORM HER-2 DISH assay shows excellent concordance with FISH assay for these most challenging (IHC 2+) breast cancer cases. Even for discordant cases, the HER2:Chr17 ratios remain within margin of error for either (FISH or DISH) assays. The presence of HER2 amplification in 100% of IHC 3+ cases suggests that false negative rate for DISH is close to negligible. DISH is performed under bright-field microscopy where the tissue morphology is better appreciated and additionally it is less expensive and faster than FISH. Our study provides strong evidence for replacing FISH with DISH assay.

2052 Use of Virtual Microscopy for the Examination of Peripheral Blood Smears at Remote Locations

J Gomez-Gelvez, D Chabot, J Arias-Stella, K Foucar, K Inamdar, K Karner. Henry Ford Hospital, Detroit, MI; University of New Mexico, Albuquerque, NM.

Background: Evaluation of the peripheral blood smear (PBS) is still essential in current medical practice. The introduction of virtual microscopy (VM) has enabled the interpretation of PBS at remote locations. In this study we aimed to validate the use of VM for the evaluation of PBS as an option to provide expert interpretation to remote sites.

Design: We selected 20 PBS representing normal and abnormal findings seen at a community-based hospital. Two hematopathologists evaluated each case using conventional light microscopy (LM) and VM by an Aperio ScanScope and ImageScope software (Aperio, Vista, CA). Reviewers (RV) were provided the patient's age, sex, brief clinical history and CBC data. Each RV performed manual differential, quantitative interpretation and morphologic evaluation of white blood cells (WBC), red blood cells (RBC), and platelets (PLT). RBC findings were graded as 0, 1+ or 2+, depending on percentage of abnormal cells. For the morphologic evaluation of WBC and PLT, all findings were registered as either present or absent. Final diagnoses were written in a free text format and compared for major (e.g. differences in the main findings) and minor (e.g. differences in the interpretation of the possible etiology of the main findings) inter- and intraobserver discrepancies.

Results: On average for the two RV, differences of >15% in the differential count was seen in 3/20 (15%) of cases for neutrophils, in 2/20 (10%) for lymphocytes and 0.5/20 (2.5%) for monocytes. None of the 20 cases showed relevant differences in RBC, WBC and PLT morphology. Comparison of final diagnoses between VM and LM showed minor discrepancies in 2.5/20 (12.5%) of the cases on average for the two RV. Interobserver comparison of LM showed minor discrepancies in 4/20 (20%) of the cases and major discrepancies in 1/20 (5%). Interobserver comparison of VM showed minor discrepancies in 1/20 (5%) of the cases and major discrepancies in 1/20 (5%), same case as in LM. Major discrepancy was due to the failure to identify a scant amount of blast cells by one of the reviewers. Reviewers agreed upon the limited analysis of intracellular inclusions, parasites and specific morphologic features.

Conclusions: VM is a useful tool in the triage of urgent specimens as an option to obtain expert interpretation in locations where experienced staff is not available on site. RBC, WBC and PLT morphology can be reliably identified. VM would be less useful for the identification of intracellular parasites and other inclusions.

2053 Reduction of Sequence Artifact in Formalin Fixed Paraffin Embedded Tissue Using Uracil DNA Glycosylase: A Comparative PCR High Resolution Melting Curve Analysis

JA Halfacre, JM Gale, MA Vasef. University of New Mexico, Albuquerque, NM; TriCore Reference Laboratories, Albuquerque, NM.

Background: Sequence artifact is occasionally detected in DNA obtained from formalin fixed paraffin embedded (FFPE) archival tissue. The sequence artifacts include C>T/G>A and is thought to be due to cytosine deamination to uracil. Although the sequence artifacts in DNA from FFPE tissue is not reproducible, it might potentially lead to errors including false positive results when using high resolution melting (HRM) curve assays for detection of mutations in genes such as KRAS, BRAF, and EGFR to determine efficacy of targeted therapy. In this study, we examined the effects of uracil DNA glycosylate (UDG) treatment in reducing C>T/G>A sequence artifacts.

Design: DNA extracted from FFPE tissue sections of histologically documented lung adenocarcinoma (51 samples) and gastrointestinal stromal tumors (3 samples) were examined for exons 18, 19, 20, and 21 of EGFR and exons 9 and 11 of GIST cases respectively with and without UDG incubation prior to parallel PCR amplification. For UDG treatment, the DNA samples were incubated with this enzyme at 37 degree Celsius

for 30 minutes before the PCR amplification. Next, the PCR amplified products were melted using high resolution melt (HRM) technique (Idaho Technology). The melting curves of UDG treated and UDG untreated samples were then compared with melting curves of known positive and negative controls.

Results: Wild type (WT) samples with severe shouldering artifact that raised the possibility of mutations were identified in approximately 5% of DNA samples without UDG treatment. However, the shouldering artifact was not present on melting curves of the parallel samples that had been treated with UDG as illustrated in Figure 1.

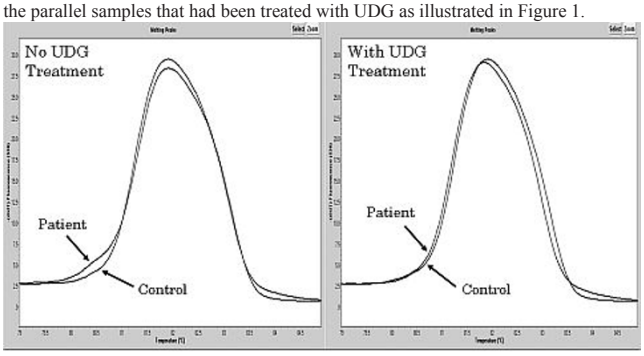

Conclusions: Incubation of DNA extracted from FFPE tissue with UDG significantly improve the shouldering artifact on melting curve assays used for mutational analysis of genes with available targeted therapy such as KRAS, BRAF, KIT, and EGFR. Treatment of DNA with UDG prior to amplification and melting analysis improve sequence artifact and reduces potential false positive results.

2054 Clinical Laboratory Validation of an Improved Flow Cytometry Assay for Detection of ZAP-70

EH Hart, M Liew, S Hill, RA Mohl, TW Kelley, DW Bahler. University of Utah and ARUP Laboratories, Salt Lake City, UT.

Background: Expression of ZAP-70 by chronic lymphocytic leukemia (CLL) is associated with a more aggressive disease course and with cases that express unmutated immunoglobulin heavy chain variable genes segments (VH). In theory, flow cytometric detection of ZAP-70 offers many advantages over other methodologies, but has not been standardized and typically shows poor reproducibility among different laboratories. We recently described a novel flow cytometric method for detecting ZAP-70 that employs an experimentally optimized isotypic control antibody (Clinical Cytometry 2012, 82B:78-84) that shows a very high degree of correlation with IgVH mutational status and generates a bimodal distribution of ZAP-70 values among CLL cases. This study examines how this assay performs in a clinical laboratory setting.

Design: All cases sent to ARUP laboratories for both ZAP-70 analysis and VH mutational status testing since November 2008 were identified. Cases submitted for ZAP-70 analysis with cell viabilities less than 95% were excluded. ZAP-70 and VH mutational status results were reviewed for the remaining cases.

Results: ZAP-70 expression among the 110 identified cases showed a discontinuous almost bimodal distribution, with the majority of cases being either in the ZAP-70 low to negative group (38) or ZAP-70 positive group (65). Expression of ZAP-70 was highly correlated with mutational status since 35/38 ZAP-70 low to negative cases had mutated VH genes and 57/65 ZAP-70 positive cases had unmutated VH genes.

Conclusions: Use of our optimized isotypic control method for setting a negative threshold to determine ZAP-70 positivity works well in a clinical flow cytometry laboratory setting and still generates a higher degree of correlation with IgVH mutational status compared to other methods. The discontinuous distribution of ZAP-70 values generated could increase the reliability of flow based ZAP-70 detection among labs and improve prognostic value.

2055 The Detection of Clonal Evolution in Acute Myeloid Leukemia (AML) Using SNP/CGH Microarray Analysis

L Hartmann, CF Stephenson, KR Johnson, DB Chapman, RK Bennington, WK Fritschle, L Eidenschink, DA Wells, MR Loken, ME de Baca, BK Zehentner. HematoLogics, Inc., Seattle, WA.

Background: Single nucleotide polymorphism (SNP) arrays were originally used for genome wide association studies. Of recent interest is SNP array analysis in the context of hematopoietic malignancies. SNP arrays have several advantages over more routine tests (metaphase analysis and fluorescence in situ hybridization [FISH]) as the genome can be evaluated at the submicroscopic level in its entirety with a single assay. SNP arrays detect copy number gains and losses, provide genotype information and allow identification of allelic imbalances such as copy number neutral loss of heterozygosity (cnLOH). SNP arrays are of limited use, however, in the identification of low-level mosaicism. [/underline] In the 8 AML case studies presented here, we demonstrate how manual re-analysis of initial microarray data can achieve improved resolution of the clonal composition, confirming the presence of clonal sub-populations as well as clonal evolution.

Design: DNA from 8 bone marrow aspirates with acute myeloid leukemia were investigated for the presence of genomic aberrations using the Agilent SurePrint G3 180K Cancer CGH+SNP microarray. Data was analyzed with the Agilent CytoGenomics software. After initial characterization of the major clone abnormalities, manual 'peak re-assignment' analysis was performed to reveal aberrations harbored by a minor clone. Findings were compared with results from interphase/ metaphase FISH studies and conventional cytogenetic analysis.

Results: Several indicators for clonal heterogeneity were detected in the SNP/CGH microarray data set for 8 AML bone marrow specimens. A difference in log2 ratios of separate chromosomal abnormalities was detected in all cases. The log2 ratios were used for manual peak assignment to determine new analysis parameters for the major and the minor cell populations. In addition, several specimens revealed a discordance of SNP calls to CGH analysis and/or complex copy number peak assignment plots as further indication for clonal heterogeneity. Distinct abnormalities could be separately extracted for minor and major cell populations when re-analyzing the SNP/CGH microarray data for all ten AML cases. FISH and/or conventional cytogenetic analysis was also used to confirm and further characterize clonal evolution in all 8 specimens. [/underline]

Conclusions: SNP/CGH array analysis allows for additional characterization of clonal sub-populations and, therefore, demonstration of clonal evolution. This is a valuable asset for the clinical work-up of hematopoietic neoplasms since clonal evolution is associated with disease progression and adverse clinical outcome.

2056 KRAS/BRAF Mutations in Colorectal Carcinoma. A Comparative Study between Real-Time PCR, Sanger Sequencing and Chip-Hybridization PCR Based Technology

J Hernandez-Losa, R Somoza, R Mares, E Lindo, A Solsona, T Moline, S Landolfi, S Ramon y Cajal. Hospital University Vall d´Hebron, Barcelona, Spain; Vall d´Hebron Research Institute, Barcelona, Spain.

Background: KRAS mutation testing is mandatory before prescribing anti-EGFR mAbs in the treatment of advanced colorectal cancer. Other studies suggest that BRAF mutation could also be relevant in the management of those patients. Sanger sequencing have been established as a Gold Standard method, nevertheless recently several methods have been described to determine those mutations. We compare a new Cancer Mutation Array kit with two well established methods in a series of 200 human carcinoma samples.

Design: We have compared three methods for mutation detections in KRAS and BRAF genes in 200 human colorectal carcinoma samples.We used two different sample sets.To assess the KRAS mutation status we used a kit based on real-time PCR (Therascreen® KRAS mutation kit,Qiagen), and a kit based on PCR amplification and array-hybridization with different probes (CLART® CMA KRAS-BRAF kit,Genomica SAU) in 159 samples. In the BRAF set we used Sanger Sequencing with specific primers of BRAF and the above mentioned CMA kit in 41 samples. The CMA kit detects 9 KRAS mutations (all G12 variants, G13D, Q61H and Q61L) and 2 BRAF mutations (V600E and V600K). DNAs were extracted from FFPE tissue samples. We compare the sensitivity of each method with several plasmids, and cell lines.

Results: The CMA kit detected KRAS and BRAF mutations in less than 5% of DNA mutant in a background of wild type DNA. Therascreen kit detected 67% (108/159) KRAS mutants whereas CMA kit detected 66% (105/159). In the BRAF set, both Sequencing and CMA kit detected 34% (14/41) of BRAF mutants.Discordant cases were analyzed in a second extraction. One G12V detected by Therascreen kit was demonstrated being a false positive in the second round by all methods. G12A and G12V sample mutants detected in both extractions by Therascreen kit were unable to be reproduced by other technologies, probably due to a lower sensitivity in these assays. Furthermore using CMA kit we detected 3 samples with KRAS and BRAF mutations that had been missed in the first analysis. In the KRAS set we detected two V600E samples and we also detected a G12C in the BRAF set.

Conclusions: The new CMA kit detects simultaneously the most prevalent mutations of KRAS and BRAF with high sensitivity and reproducibility in 2 steps. The concordant results obtained by CMA kit compared to a well established methods supports the use of this technology in different screenings to testing KRAS and BRAF mutations in human colorectal cancer samples.

2057 Retrospective Review of Emergent Frozen Sections at a Large Teaching Hospital

MD Hyrcza, NE Sunderland, CB Gilks. University of British Columbia, Vancouver, BC, Canada; Vancouver General Hospital, Vancouver, BC, Canada.

Background: Unexpected, emergency frozen section is one the anatomic pathologist's most demanding and stressful tasks, yet residency training programs do not systematically prepare young pathologists for this difficult task. Emergency frozen sections are infrequent and tend to involve a distinct set of conditions, different from the usual types of specimens received for frozen section analysis. Review of literature reveals a dearth of published data on this topic. Specifically, the frequency and types of specimens submitted for emergent frozen sections are have not been reported in recent publications.

Design: We retrospectively analyzed the emergency frozen sections performed on weekends for non-neuropathology cases at Vancouver General Hospital, a large metropolitan teaching hospital, between June 2010 and Aug 2012. Eighteen cases were identified for which the on-call pathologist was requested to perform emergent frozen section analysis.

Results: The indications for the emergent frozen sections were: diagnosis (lesion identification) in 13/18 cases (72%), margin assessment in 2/18 cases (11%), and transplant tissue quality assessment in 4/18 cases (22%) (one case involved both margin and diagnosis). Of the eighteen cases, six (33%) were performed for emergent general surgery cases such as perforated or obstructed viscus, severe bleeding from a mass, and one case of VIPoma causing severe hypokalemia. Four cases (22%) involved assessment of liver biopsies for steatosis prior to a cadaveric liver transplant. Four cases (22%) involved mediastinal lesions causing either superior vena cava syndrome or acute cardiac symptoms. Three cases (17%) involved orbital or base of skull masses. The final case involved acute spinal cord compression (6%).

Conclusions: The review of emergent frozen sections revealed a distinct set of situations for which emergent frozen section analysis is called for. These include: 1) acute presentations of gastrointestinal mass lesions causing obstruction, perforation, bleeding

or other symptoms requiring same day surgery; 2) mediastinal masses causing SVC syndrome or acute cardiac symptoms; 3) orbital or skull base masses presenting with acute vision loss or other neurological deficits; 4) spinal cord compression syndrome; and 5) assessment of liver biopsies for steatosis prior to a liver transplant. Identifying these classes is the first step to development of an educational program to specifically prepare pathology residents for this challenging responsibility.

2058 Tissue Microarray Advanced Techniques for Sampling Donor Blocks with Limited Tissue: The "Radical Tissue Microarray"

T Jensen, DV Miller, D Nilson, M Cessna. Intermountain Healthcare, Salt Lake City, UT.

Background: Tissue Microarrays (TMAs) are increasingly used in pathology; economizing reagents, space, and interpretive time. High quality tissue arrays depend on donor blocks with adequate tissue. We report the use of advanced techniques that can be used to salvage tissue for TMA construction from blocks with limited tissue.

Design: We have developed strategies to maximize the yield of tissues from donor blocks in TMA construction. Two such techniques are outlined and illustrated according the nature of the sample limitation.

Results: Scraping Technique: Small tissue (e.g. needle biopsies) or tissie scattered throughout the donor block can be collected for TMA construction using the scraping technique. Using a marked H&E slide as a roadmap, tissue can be scraped from the donor block using a scalpel tip. The tissue scrapings can be carefully transferred to a skin biopsy punch whose diameter has been matched to permit the stylet from another TMA coring device (e.g. a 2mm skin punch with a 2mm stylet). The haphazard tissue scrapings are tamped down into the skin biopsy punch using the stylet and the resulting tissue "sausage" embedded in paraffin. Larger bore "sausages" can be sampled multiply by smaller bore coring devices (see figure). Perpendicular Stacking Technique: Tissue form nearly exhausted blocks (large surface area but shallow depth) can also be collected for TMA construction using the perpendicular stacking method. The paraffin block is melted and the remaining tissue wafer cut into several ~0.5 cm squares. The squares are stacked then the stack turned on end and embedded. Cores can then be punched from vertically stacked tissue for use in TMAs (see figure). Because the TMA cores resulting from these techniques are slightly more fragile than solid tissue cores, It is recommended that the TMA coring device be used to punch a piece of thin cardboard just prior to coring a scraped or stacked tissue specimen. This will allow the cardboard to act as a barrier, protecting the tissue from indentation by the stylet.

Conclusions: Though limitations in donor tissue blocks present a challenge to high quality TMA construction, the scraping and perpendicular stacking techniques can be employed to increase the yield from limited blocks.

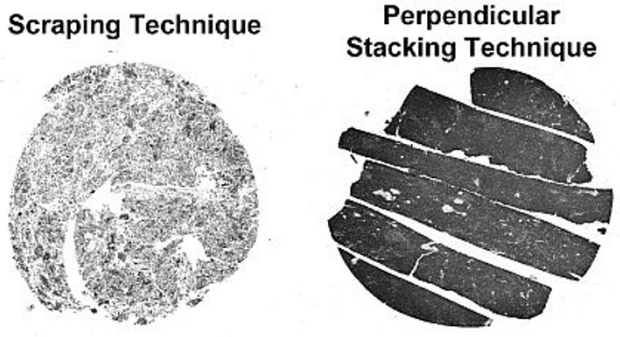

2059 Validation of Prognostic Biomarkers on Prostate Cancer Tissue Microarrays

AD Johnson, AE Rizzardi, LO Marston, JS Koopmeiners, GJ Metzger, CL Forster, RI Vogel, JB McCarthy, EA Turley, JR Tiffany, Z Ronai, CA Warlick, SC Schmechel. University of Minnesota, Minneapolis, MN; NCI-Designated Cancer Center, San Diego, CA; University of Western Ontario, London, ON, Canada.

Background: Biomarkers that predict disease aggressiveness leading to prostate specific antigen (PSA) failure after prostatectomy may facilitate selection of adjuvant therapies. We assessed the prognostic value of 33 biomarkers using immunohistochemistry (IHC) on tissue microarray (TMA) sections representing PCa tissue from prostatectomies of 153 patients for whom clinicopathologic features and PSA follow-up after surgery were available.

Design: Potential prognostic biomarkers were assessed based on RNA expression profiling, data analysis and literature review. Using a cross-study data analysis we have selected 11 genes (ACPP, ADAM9, ALDH1A2, CASR, CCPG1, GADD45B, HOXC6, IGF1, IQCK, PAGE4 and PLIN2) that best distinguished aggressive (leading to PSA failure after prostatectomy) versus non-aggressive PCa. 4 additional genes (CHMP1A, EI24, MAP4K4, and MKI67) were selected based on published expression analyses. Additional biomarker candidates, based on literature review, included 6 associated with hyaluronan (HA) processing (HA, HAS2, HMMR, HYAL1, CD44, and CD44v6), 7 implicated in prognosis of PCa (CCND1, PTEN, SMAD4, SPP1 [PMID:21289624]; HES6, SIAH2, and SOX9 [PMID:20609350]), 3 neuroendocrine markers (CHGA, NSE, SYP), an angiogenesis marker CD34, and the tumor suppressor p53. Software algorithms (Genie Histology Pattern Recognition and Color Deconvolution, Aperio) were used on whole slide images of stained TMAs to automate tissue annotation into several classes (tumor, stroma, and empty glass) and quantify IHC staining. Hazard ratios associating increased expression with decreased time to biochemical failure were calculated.

Results: Established pathologic parameters were each separately associated with time to PSA failure. In tumor areas, IHC expression of CCND1, HMMR, IGF1, KI67, SIAH2 [nuclear], and SMAD4 were separately associated with shorter time to PSA failure. After adjustment for adverse clinicopathologic features HMMR, HOXC6, IGF1, MAP4K4, and SMAD4 were independently associated with shorter time to PSA failure. Notably, 3-gene signature (HMMR, SIAH2 [nuclear], and SMAD4) had the best n-gene performance with AUC 0.721 for 5-year PSA failure (p=0.002).

Conclusions: We identify that expression of CCND1, HMMR, HOXC6, IGF1, KI67, MAP4K4 and SIAH2 [nuclear] were associated with shorter time to PSA failure. Further, a 3-gene model (HMMR, SIAH2 [nuclear], and SMAD4) appears to serve as a useful signature associated with shorter time to PSA failure.

2060 Assessment of BRAF V600E Mutation Status by Immunohistochemistry in Lung and Ovarian Carcinomas

OE Kabiawu-Ajise, JT Feldstein, R Soslow, D Levine, M Ladanyi, ME Arcila. Memorial Sloan-Kettering Cancer Center, New York, NY.

Background: BRAF mutations are implicated in the pathogenesis of several cancers, including melanoma, lung adenocarcinoma (ADC), colorectal cancer (CA), thyroid CA, ovarian CA and hairy cell leukemia. The V600E mutation is the most common and is emerging as an important biomarker of prognostic and therapeutic significance. While the BRAF mutation status is most commonly determined by DNA-based methods, the use of immunohistochemistry with a mutation-specific antibody has been recently described in thyroid CA, melanoma and hairy cell leukemias as a highly reliable and cost effective method of screening. Its application in lung ADC and ovarian CA, where the V600E mutation is less frequent, (~[/underline]2% and 11%, respectively), is not well described.

Design: We evaluated the performance of the BRAF V600E mutation-specific antibody (clone VE1) in molecularly characterized ovarian serous carcinomas and lung adenocarcinomas. Paraffin embedded tissue blocks were obtained from 154 surgically resected lung adenocarcinomas and 67ovarian serous carcinomas. Tumor samples were prepared in tissue microarrays and stained by immunohistochemistry with the BRAF V600E mutation-specific antibody, clone VE1. Whole tissue sections were analyzed in 16 cases. The pattern of expression was graded based on intensity of cytoplasmic staining in a 0 to 3+ scale and results were correlated with the mutation status as determined by standard DNA-based molecular methods.

Results: A total of 18 *BRAF* V600E mutated cases had been identified by molecular testing (10 lung, 8 ovary). The staining intensity in *BRAF* V600E mutated tumor samples ranged from weak (1+) to strong (3+). In lung adenocarcinomas, IHC with the VE1 antibody showed a sensitivity of 60% and a specificity and positive predictive value of 100% using a positivity cut off of 2+. In ovarian tumors, the sensitivity reached 88% with specificity and PPV of 100%. Non-specific, weak and diffuse cytoplasmic staining was identified in 85% and 89% of lung and ovarian cases, respectively, precluding the use of a 1+ cytoplasmic staining cutoff for positivity. Non-specific nuclear staining was also identified in some cases.

Conclusions: Immunohistochemistry using the VE1antibody to BRAF V600E could be used to establish the BRAF mutation status in ovarian and lung carcinomas. However, compared to other malignancies, the sensitivity is lowered by the non specific cytoplasmic staining imparted by mucinous or serous components within these tumors, and therefore negative staining results would not eliminate the need for BRAF mutation analysis, if clinically indicated.

2061 Comparison of FFPE DNA Extraction Methods Using a Molecular Pathology Assay

S Kip, J Winters, K Rumilla, B Kipp. Mayo Clinic, Rochester, MN.

Background: With the implementation of recent FDA approved companion diagnostic tests, some laboratories are required to validate additional xylene deparaffinizing extraction methods. Our laboratory has the Roche cobas® DNA Sample Preparation Kit (cobas) and the Qiagen QIAamp® DSP DNA FFPE Tissue Kit (DSP), in addition to the Qiagen QIAcube DNA extraction method. Since many cancer patients have limited specimen and require multiple tumor marker tests, our aim was to cross validate these techniques for molecular pathology testing.

Design: We analyzed 11 FFPE tumor samples that were originally ordered for clinical KRAS testing. Using the same amount of macrodissected tissue, DNA was extracted using the 3 methodologies and tested using the Qiagen therascreen® KRAS RGQ PCR Kit. This KRAS assay consists of a control reaction and seven mutation reactions. The crossing threshold (C_T) value of the control reaction provides a metric for of the amount of amplifiable DNA, which is then compared to the C_T values of the mutations reactions to determine mutation status. The C_T value of the control reaction was compared between extraction methods for each of the 11 cases. There were 6 KRAS positive cases and their C_T mutation values were compared between extraction methods. Final KRAS mutation status was also compared.

Results: The QIAcube method's control reaction's C_T values ranged from 23.75 to 27.65; the Cobas method's values ranged from 21.54 to 26.46; and the DSP method's values ranged from 23.16 to 27.71. Of these 33 separate analyses, 32 had an acceptable C_T values (21.92 to 32.00). One cobas extracted sample had too much DNA and had to be diluted. The %CV between extraction methods (control reaction's C_T values) ranged from 0.3% to 6.2%. For the 6 positive cases, the %CV between extraction methods (mutation reaction's CT values) ranged from 1.9% to 8.2%. The final mutation results of the 11 cases were concordant for all three methodologies.

Conclusions: The results of this study indicate that the DNA extracted by any of these methods is acceptable for use with the therascreen® KRAS RGQ PCR Kit. For specimens with only enough tissue for one DNA extraction, cross validating extraction methods is necessary for testing additional markers. However, for some FDA approved assays, the different extraction method may be considered "off label" use based on current regulatory guidelines. However, the flexibility of using quality DNA from different extraction methods would likely reduce the need for multiple

DNA extractions, reduce cost, and reduce the amount of tissue needed to perform these important clinical tests.

2062 Level of Agreement between Paired Paraffin and Frozen Renal Tumor Samples on SNP Microarray

S Koo, A Minor, P Reddy, T Antic, L Joseph, C Fitzpatrick, M Tretiakova. University of Chicago, Chicago, IL.

Background: Copy number alterations occur in many solid tumors including renal cell carcinomas (RCC), which can be classified due to distinctive chromosomal abnormalities. Single nucleotide polymorphism (SNP) microarrays may be useful for RCC characterization, as they provide whole-genome copy number data at higher resolution and can detect copy number-neutral loss of heterozygosity (LOH). While there have been advances in utilizing SNP microarrays in formalin-fixed paraffin-embedded (FFPE) tissue, few comparisons between results from FFPE tissue and fresh-frozen (FF) tissue have been made, and none of those studies investigated paired RCC samples.

Design: Paired, morphologically matched FF and FFPE tumor tissues were obtained from five RCC specimens, including clear cell, papillary, and chromophobe subtypes. Genomic DNA was quantitated using Picogreen, assessed for integrity using gel electrophoresis, and processed according to the standard protocol for Affymetrix Genome-Wide Human SNP Array 6.0. Acquired data were analyzed for copy number changes (CNC) and LOH using the Affymetrix Chromosome Analysis Suite.

Results: Following previously published optimization steps for FFPE samples, including increased amount of starting DNA, number of PCR cycles and DNase fragmentation time, CNC and LOH were compared for FFPE and matched FF samples. Results are summarized in the table.

	Identified in both FFPE and FF	Identified in FFPE, not FF	Identified in FF, not FFPE	% agreement
Normal copy number	85	0	2	98%
Overall CNC	13	4	10	48%
Whole/partial chromosome gain/loss	9	4	7	45%
Mosaic gain/loss	4	0	3	57%
LOH	0	0	4	0%

While agreement between FFPE and FF tissue is excellent (98% agreement) for chromosomes where the copy number is unaltered, agreement is significantly decreased with CNC (48%). Specifically, SNP genotype data from FFPE samples were difficult to interpret, while SNP data from FF samples were readily interpretable and were used in multiple cases to confirm or reject apparent CNC. The most difficult-to-interpret CNC were whole chromosome gains and losses. Similarly, LOH could not be detected in the FFPE samples.

Conclusions: Although SNP microarrays on FFPE samples can provide useful genetic information, the overall agreement for CNC between FFPE and FF RCC samples is less than 50%. This low degree of agreement can be problematic for cytogenetic analysis and diagnosis for these tumors if only paraffin tissue is available. In an effort to improve data quality, we plan to expand the scope of this study in more cases using higher-resolution SNP microarrays and an FFPE-specific reference set for data analysis.

2063 Performance Studies of the New One-Day *HER2* IQFISH PharmDx™ – European Multicentre Experience

M Lacroix-Triki, D Hardisson, MG Tibiletti, C Franchet, F Penault-Llorca, J Jacquemier, G Mac Grogan, L Arnould, T Garcia-Caballero, A Concha, G Viale, J Ruschoff. Institut Claudius Regaud, Toulouse, France; University Hospital La Paz, Madrid, Spain; Ospedale di Circolo-University of Insubria, Varese, Italy; Centre Jean Perrin, Clermont-Ferrand, France; Institut Paoli Calmettes, Marseille, France; Institut Bergonié, Bordeaux, France; Centre GF Leclerc, Dijon, France; University Hospital, Santiago de Compostela, Spain; University Hospital Virgen de las Nieves, Granada, Spain; Institute of Oncology and University of Milan, Milan, Italy; Targos Molecular Pathology gmbh, Kassel, Germany.

Background: *HER2* IQFISH pharmDx™ is a direct fluorescence in situ hybridization (FISH) assay developed with a new non-toxic buffer which reduces hybridization time to only 1-2 hours, enabling a turnaround time of only 3h30min from dewax to counting. We report herein the results of several independent European studies comparing the new IQFISH assay to existing in situ hybridization (ISH) assays.

Design: Comparison studies were independently performed in Germany (one centre), France (five centers), Spain (three centers), Italy (one centre). Cases included in the studies (range, n=27-200) consisted of invasive breast and gastric carcinomas, selected according to HER2 IHC status. *HER2* IQFISH pharmDx™ was compared with *HER2* FISH (pharmDx™ or PathVysion® *HER-2* DNA probe kit) in all studies, Inform Her2 Dual ISH (DISH) (one study) or duoCISH™ (one study). *HER2* gene and *CEN17* copy number, *HER2/CEN17* ratio, staining quality, success rates, handling and workflow were recorded. Among the 4 studies, one was performed on tissue microarrays and several fixatives were tested.

Results: *HER2* IQFISH pharmDx™ showed a high level of concordance with FISH (concordance rates from 96.3% to 100%, k=0.914 to 1.00), DISH (96%, k=0.877) or duoCISH™ (94.7%, k=0.875). Failure rates ranged from 2-7% for IQFISH, as compared with 1-9% for FISH, 5% for DISH and 9% for duoCISH™. IQFISH quality was assessed as optimal with brighter nuclei (DAPI), allowing an easy orientation in tissue at low magnification, and more intense red and green signals as compared to FISH. Discordant cases were mainly tumours in the borderline category or so-called polysomic cases, and rarely true heterogeneous tumours.

Conclusions: *HER2* IQFISH pharmDx™ is a new high-quality non-toxic assay showing high concordance rates with other in situ hybridization techniques. With a turnaround time of 3½ hours, it improves the workflow and allows a fast *HER2* status assessment useful for daily clinical practice and enrollment of patients in targeted clinical trials.

Abstract #2064 has moved to Bone and Soft Tissue

2065 New Visualization Technique Enables Her2 Immunofluorescence Staining To Resemble Traditional Chromogenic DAB Stain

M Lazare, K Kenny, N Jun, A Kyshtoobayeva, D Hollman, D Henderson, A Corwin, T Ha, S Kaanumalle, C McCulloch, K Bloom. GE Global Research, Niskayuna, NY, Vanuatu; Clarient Diagnostics, a GE Healthcare Company, Aliso Viejo, CA.

Background: The current clinical method for testing Her2 status involves using chromogenic immunohistochemistry (IHC) to detect Her2 protein expression. Chromogenic stains have several limitations that can be overcome by using immunofluorescence (IF). IF allows for the collection of linear, quantitative data across a greater dynamic range than chromogenic stains, which is particularly useful for Her2. However, conventional IF images can be difficult for pathologists to read compared to the commonly accepted, high contrast, chromogenic stains such as DAB. Here, we demonstrate the ability to convert traditional grayscale IF images into "molecular DAB" (mDAB) images which simulate the appearance of true DAB. This gives the pathologist the benefits of IF while making the images as readable as a chromogenic stain.

Design: IF and DAB staining was performed on 12 FFPE invasive ductal breast carcinoma samples that exhibited varying degrees of Her2 expression, collected between June 2011 and March 2012. A mAb for Her2 was used for conventional DAB staining. The same antibody was conjugated to Cy5 dye for IF staining on serial sections. Two board-certified pathologists scored both the mDAB and DAB images on a 0/1+/2+/3+ scale. In each patient where mDAB & DAB scores were discordant, alterations in Herceptin treatment recommendations were recorded in light of the patient's clinical Her2/CEP17 amplification ratios via FISH.

Results: Pathologists 1 and 2 had consistent scoring between mDAB and DAB in 8/12 cases (kappa=0.29) and 10/12 cases (kappa=0.68), respectively. The two pathologists agreed in 12/12 mDAB images (kappa=1) but only 8/12 DAB images (kappa=0.29). Of the 5 cases of discordance between mDAB & DAB for either pathologist, 3 would have been given the same Herceptin recommendation based on the mDAB or the DAB scoring. In one case the mDAB score would have led to Herceptin treatment of a case with confirmed Her2 gene amplification via FISH, while the DAB scores would not have resulted in Herceptin treatment. FISH data was not available in the last discordant patient. It is noteworthy that there were no discordant cases among the mDAB reads.

Conclusions: Immunofluorescence staining offers many technical advantages over traditional brightfield immunohistochemistry. Despite these advantages, interpretation of raw darkfield images can be challenging. Therefore, this molecular DAB technique offers a promising method for rendering IF images in a manner more familiar to pathologists; therefore combining the best of both worlds.

2066 Novel Image Processing Technique Allows Immunofluorescence Signals To Resemble Traditional H&E Stain and Enable Multiple Biomarker Visualizations on a Single Slide

M Lazare, K Kenny, N Jun, A Kyshtoobayeva, D Hollman, D Henderson, A Corwin, T Ha, C Chow, K Bloom. GE Global Research, Niskayuna, NY; Clarient Diagnostics, a GE Healthcare Company, Aliso Viejo, CA.

Background: The current protocol for examining a sample via immunohistochemistry involves using one section of tissue for a chromogenic stain to visualize a single biomarker of interest and another serial section for hematoxylin and eosin (H&E) staining to visualize the morphology of the tissue, identify tumor, and determine regions of interest (ROI). Some of the limitations of using two slides are that 1) tissue can be limited and cutting a second slide for an H&E may exhaust available tissue, precluding further chromogenic tests, and 2) since the stains are on separate slides it can be difficult to correlate fields of view of the two stains. Here, we describe a method to use immunofluorescence (IF) staining and autofluorescence (AF) for morphology determination and ROI selection which will allow the same slide to be used for target biomarker staining as well. We have termed this technique "molecular H&E" (mH&E).

Design: Slides were stained with DAPI, a cy3 conjugated pan-cytokeratin antibody, and a cy5 conjugated Her2 antibody. IF whole slide imaging was then performed using filters for DAPI, FITC, Cy3, and Cy5. Image processing techniques were used to blend the DAPI (nucleus), FITC (AF), and Cy3 (epithelium) images to closely resemble an image of a true H&E stain. A board-certified pathologist reviewed 21 breast cancer cases using mH&E images initially, followed by true H&E images of serial sections of the same case series. The pathologist assessed the images based on two main scoring categories: the ability to 1) identify normal tissue, stroma, ductal carcinoma in situ (DCIS), and invasive tumor, and 2) to assess tissue percentage of invasive tumor.

Results: The pathologist was able to identify the stroma and invasive components in all samples using either type of H&E. Of the 18 cases where normal tissue was observed in the H&E, 15 cases had normal tissue detectable via mH&E. Of the 13 cases where DCIS was observed in the H&E, 11 DCIS cases were detected via mH&E. There was consistently ≤ 20% difference between the two tumor percentage scores.

Conclusions: Variability of tissue between serial sections likely contributed to some observed discrepancies. Overall the pathologist was satisfied with the mH&E as compared to the traditional H&E. Importantly, Her2 was also stained in Cy5, which facilitated side-by-side display of mH&E images and Her2 to visualize these two distinct pieces of information on the same slide.

2067 Comparative Analysis of Different Types of KRAS Mutation between Frozen and Paraffin Embeded Tissue Using the Pyrosequencing Method

MP Macedo, FM Mello, BCG Lisboa, LDB Andrade, AHJFM Campos, DM Carraro, FA Soares, IW Cunha. Hospital A.C.Camargo, São Paulo, Brazil.

Background: *KRAS* mutation is a negative predictor of response to treatment with Epidermal Growth Factor receptor inhibitors and is detected in ≈35% of Colorectal Carcinomas (CRC). KRAS mutation analysis is performed in routine practice in formalin fixed and paraffin embedded tissue (FFPET). Formalin fixation has been described to induce artifact mutations in selected genes, mostly due to error in DNA pairing during sequencing procedures. Some studies have compared KRAS status between FFPE and frozen tissue, but mostly regarding KRAS status (wild versus mutated). The objective of this study is to examine whether the detection of the most frequently described types of KRAS mutations found in CRC are reproducible between FFPET and frozen tissue using the pyrosequencing method.

Design: Twelve previously sequenced FFPET from CRC cases mutated for KRAS gene were selected based on the type of mutation detected and the availability of paired frozen tissue in Hospital A.C.Camargo Biobank. DNA from FFPET was extracted using the QIAmp DNA Extraction Kit; DNA from frozen tissue was extracted using an in house technique. PCR was performed with 100 ng of DNA, targeting the regions containing codons 12 and 13 using the KRAS PyroMark™ Q24 kit (Qiagen). Pyrosequencing reaction was performed using the manufacturer's instructions (KRAS PyroMark™ Q24 V2.0 (Qiagen).

Results: The twelve study cases consisted of seven tumors mutated in codon 12 and 5 in codon 13. Mutations in codon 12 were GGT>GAT (3 cases), GGT>GTT (3 cases), GGT>AGT (1 case). All mutations in codon 13 were GGC>GAC. The pyrosequencing using the DNA from the paired frozen tissue showed 100% of compatibility regarding the mutations detected in the FFPET.

Conclusions: KRAS mutation detection by pyrosequencing DNA from FFPET is highly reproducible with DNA from frozen tissue. This study shows no negative impact of formalin fixation in the detection of the most common types of KRAS mutation in CRC by pyrosequencing method.

2068 Evaluation of Two Molecular Methods for Genotyping FCGR3a in Non Hodgkin Lymphoma Patients

S Malhotra, PR Burchard, P Kaur, GJ Tsongalis. Geisel School of Medicine at Dartmouth, Hanover, NH; Dartmouth-Hitchcock Medical Center and Norris Cotton Cancer Center, Lebanon, NH.

Background: Fc receptor III A of immunoglobulin G (FcγRIIIA, also called CD16) belongs to the Fc gamma receptor family (FCGR) which plays an important role in immunoinflammatory processes. It is a low affinity, trans membrane receptor and is mainly expressed in monocytes, NK cells and macrophages. It has been implicated in various inflammatory conditions and recently a polymorphism in this gene has been shown to influence response to rituximab (anti CD20) therapy in various disorders. We evaluated two molecular methods to genotype this polymorphism.

Design: Archived FFPE samples from 30 biopsies of Diffuse Large B Cell Lymphoma were retrieved and DNA was extracted. The samples were tested for the FCGR3a polymorphism using a real time PCR followed by melt curve analysis or by a standard Taqman allelic discrimination assay using the AB 7500 FAST real time PCR instrument. The Taqman assay consisted of the following PCR conditions: 60C for 1:00; 95C for 10:00; 40 cycles of 92C for 15 sec, 60C for 1:00; 60C for 1:00.The PCR/melt curve assay was performed using the following conditions: 95C for 5:00; 40 cycles of 95C for 20 sec, 56C for 20 sec, 72C for 30 sec followed by a continuous melt from 72C for 10 sec then 1% continuous temperature increase until 97C for 10 sec.

Results: With the Taqman allelic discrimination assay, twenty cases had the homozygous wild type F/F genotype for the FcγRIIIA receptor, while two cases had the homozygous V/V polymorphism and eight cases were heterozygous with a V/F genotype. Results with the real time PCR followed by melt curve analysis were similar for twenty five cases, however four samples did not have sufficient DNA sample for the melt curve analysis method and the result from one sample was discordant.

Conclusions: The new Taqman assay offers several advantages over previously published assays such as rapid turnaround time, ease of interpretation, less sample DNA requirement and higher specificity without compromising sensitivity. These performance characteristics make it highly suitable for use in a clinical laboratory.

2069 Comparison of Breast Cancer Proliferation Rates between Core Biopsy and Surgical Excision Using Visual Mitotic Count and Automated Analysis of MIB-1 and PPH3

R McCormick, C Cohen, M Schoen, J Wang, A Adams. Emory University, Atlanta, GA.

Background: Moderate correlation in the histologic grade of breast cancer between core biopsy (CB) and corresponding surgical excision (SE) has been demonstrated, the difference often due to underestimation of mitotic count in the CB. Studies have shown better concordance with regard to proliferation rate between CB and SE using visual assessment of the immunohistochemical markers MIB-1 and PPH3. Using visual mitotic count (VMC) on SE as the gold standard, our aim is to assess whether automated image analysis of MIB-1 and PPH3 yields improved agreement with regard to proliferative rate.

Design: All breast cancer cases with available material from both CB and SE specimens were identified over a 14 month period. Cases from patients receiving neoadjuvant therapy were excluded. A VMC was performed on H&E sections for both the CB and SE, using cutoffs based on CAP protocol for microscope field diameter. Slides from the CB and SE specimens were also stained for MIB-1 and PPH3. To determine the average percentage positivity for MIB-1 and PPH3, 3 and 10 random fields, respectively, were assessed using an Automated Cellular Imaging System III (DAKO Corp) from "hot spot" fields identified at 20x. MIB-1 staining was categorized as low (<10%), intermediate (10-20%), or high (>20%). PPH3 positivity was categorized as low (<2%), intermediate (2% to 5%), or high (>5%). Results for VMC (on CB), MIB-1, and PPH3 were compared to the gold standard of VMC on SE.

Results: 28 cases were identified with both a CB and corresponding SE. Agreement between the methods is illustrated in Table 1.

Table 1. Agreement Between Various Methods of Assessing Proliferation Compared to the Visual Mitotic Count on Surgical Excision

Weighted Kappa	CB	SE
VMC	0.373	-------
MIB-1	0.063	0.129
PPH3	0.033	-0.032

VMC=visual mitotic count; SE=surgical excision; CB=core biopsy

Conclusions: Consistent with prior reports, our results show fair agreement for VMC between the CB and SE. The low rate of agreement between MIB-1 and the gold standard on both CB and SE is not all that surprising given that MIB-1 labels cells in G_1, S, and G_2 phases in addition to M phase; however, agreement is improved with use of the SE specimen versus the CB. We had predicted better agreement between the gold standard and PPH3-stained CB and SE sections (weighted kappa 0.033 and -0.032, respectively). The results are likely due to the cutoff values for PPH3 established for the automated imaging system. Investigation to further refine these values may yield improved agreement.

2070 Single Cell Manipulation Technology-Towards "Ink-Jet" Printing of Cancer Arrays

V McEneaney, H Keegan, M Gallagher, C Martin, O Sheils, J Schondube, A Gross, P Koltay, J O'Leary. Trinity College Dublin, Dublin, Leinster, Ireland; IMTEK, Freiburg, Germany.

Background: An ongoing EU Framework 7 project (PASCA: Platform for Advanced Single Cell Manipulation and Analysis) has developed a novel instrument referred to as a Single Cell Manipulator (SCM) device which enables 1) isolation of single cells from a cell suspension 2) generation of a picoliter sized droplet containing the single cell and 3) printing of the single cell in an "ink-jet" like manner in an automated, ordered array onto a chosen substrate for subsequent downstream analysis.

Design: The biological or clinical samples are injected into the silicon dispenser chip, coupled to a live cell camera that images and displays cells approaching the chip exit nozzle. An optical particle detection mechanism determines the presence of single cells within a selected region of interest, whilst a sorting algorithm ensures that only droplets containing single cells are selected for printing to the prescribed location. The SCM will be further developed within the project to allow sorting of cells based on their electrical impedance properties or with the detection of fluorescently labelled tags.

Results: Applications currently undergoing analysis on SCM technology include - but are not exclusive to – cervical cytopathology, anaplastic thyroid carcinoma and cancer stem cells. In cervical cytopathology, single HeLa cells have been printed and successfully cultured in 96 well plates. Separation of HPV negative and HPV positive cervical cells from mixed populations with subsequent printing of the isolated cells into ordered arrays is ongoing, with a view to progressing to printing arrays of clinical cytology samples onto microscopy slides. Single WT thyrocytes and anaplastic thyroid carcinoma cell lines have been successfully printed and cultured in 96 well plates. Separations of WT thyrocytes and anaplastic thyroid carcinoma cells have been performed from mixed populations on the SCM based on size properties and a 100% cell selection success rate has been confirmed with fluorescence microscopy.

Conclusions: The SCM PASCA technology allows isolation of single cells from a heterogeneous population followed by ordered automated printing of these cells onto a chosen substrate. The device is further being developed to allow the printing of cancer arrays whereby the cells in a clinical sample are spatially arranged according to a gradient of abnormality. This technology will assist in analysis of individual cells within many tumours and disease types, thus leading to a greater understanding of the complexity within clinical diagnostics and therapeutics.

2071 A Modified HER2 Image Analysis Algorithm with ASCO/CAP Criteria Has High Concordance with FISH

DM Minot, JS Voss, BR Kipp, A Dogan, RP Ketterling, AM Plagge, T Mounajjed, AC Clayton. Mayo Clinic, Rochester, MN.

Background: Pathological assessment of the HER2 protein is a key biomarker to determine trastuzumab eligibility in patients with breast cancer. Recent advancements in image analysis (IA) allow for HER2 scores to be calculated based on guideline recommendations (i.e. ASCO/CAP). In this validation study, we compared results from an FDA-cleared IA algorithm using the Ventana Pathway HER2 stain (Ventana Medical Systems, Tucson, AZ), as well as a modified HER2 IA algorithm using the FDA and ASCO/CAP staining percentage cutoffs.

Design: Slides from 142 breast cancer specimens were analyzed by HER2 IHC and FISH (PathVysion, Abbott Molecular Inc. Des Plaines, IL). These slides were analyzed using the Aperio digital pathology system (Aperio, Vista, CA). The test set (n=58) was analyzed using 2 different analysis techniques: 1)a method representing 6 areas of high, moderate and low intensity staining and 2)a whole tumor tracing method. Two IA algorithms (FDA-cleared and modified) were used to measure HER2 staining intensity and HER2 positivity (3+) was determined using ASCO/CAP and FDA cutoffs. The validation set (n=84) was analyzed using the technique and algorithm that achieved the highest concordance with FISH during the test set. Precision assessments were performed on a set of 20 previously analyzed cases.

Results: The whole tumor tracing technique with a modified IA algorithm using the ASCO/CAP cutoff had the highest accuracy when compared to FISH (100%; 58/58) (Table 1) using the test set. This method also demonstrated very high accuracy

(99%; 83/84) (Table 2) and precision (95%; 19/20) for both inter- and intraobserver measurements in the validation set. In addition, 10 cases converted from HER2 IHC (2+) to HER2 (3+) that were all FISH amplified and 15 cases were downgraded from HER2 equivocal (2+) to HER2 negative with one case being FISH amplified.

Table 1. Accuracy of Analysis Methods and Algorithms (Test Set)

Method	Accuracy (%)
6 area method (FDA -cleared)	53/58 (91)
6 area method (modified)	56/58 (97)
Whole tumor trace (FDA -cleared)	56/58 (97)
Whole tumor trace (modified)	57/58 (98)
Whole tumor trace (modified and ASCO/CAP cutoffs)	58/58 (100)

Table 2. Accuracy of HER2 IA (Validation Set)

	0	1+	2+	3+	Total
FISH Non-amplified	19	19	20	0	58
FISH Amplified	0	1	6	19	26
Total	19	20	26	19	84

Conclusions: Data from this validation study shows that modifications to the Aperio FDA-cleared HER2 analysis algorithm achieved high concordance between IA and FISH. The number of HER2 IHC equivocal cases triaged to FISH also decreased with the modified IA algorithm using the ASCO/CAP cutoffs.

2072 Array-Comparative Genomic Hybridization Detection of Previously Undetected Genomic Aberrations in Formalin-Fixed Paraffin-Embedded Myeloid Sarcoma

MK Mirza, M Sukhanova, P Reddy, L Joseph, G Raca. University of Chicago Medicine, Chicago, IL.

Background: Myeloid sarcoma (MS) is an extramedullary manifestation (EM) of acute myeloid leukemia (AML). Usually presenting as a mass lesion, MS is often not associated with a diagnosis of AML. Cytogenetic evaluation is an essential ancillary study for the accurate classification of AML. However, conventional cytogenetics is limited by the requirement for dividing cells and metaphase chromosomes. Formalin-fixed, paraffin-embedded (FFPE) material is often the only available specimen for analysis in EM AML. In recent years high resolution whole-genome array analysis has become a routine methodology in clinical testing for constitutional genetic disorders, and its utility is now being investigated for neoplastic lesions. Whole genome SNP arrays allow high-resolution, genome-wide detection of copy number abnormalities and loss of heterozygosity (LOH) events in tumor samples, using DNA isolated from either fresh or FFPE tissue. We hypothesize that SNP array analysis represents a sensitive, clinically applicable assay for detection of genetic abnormalities of diagnostic and prognostic significance in MS.

Design: Array testing was performed using CytoScan HD array (Affymetrix Inc), following the manufacturers protocol. DNA was isolated using the Qiagen DNeasy extraction protocol (QIAGEN Inc., Valencia, CA) and Flt3 ITD and D835 mutation testing was performed using a kit from InVivoScribe Technologies (San Diego, CA).

Results: We performed array analysis on a case of MS where conventional cytogenetics had revealed a trisomy 8 (karyotype: 47,XY,+8[20]). Array analysis detected the presence of +8, and additionally showed LOH for all of chromosome 13. Knowing that *FLT3* maps to chromosome 13, and that LOH may have been a mechanism to increase the dosage of a mutant *FLT3* allele in the tumor, we proceeded with testing the sample for the *FLT3* ITD and D835 mutations. Molecular testing demonstrated the presence of the D835 mutation.

Conclusions: Array analysis of this case not only detected trisomy 8 seen by conventional cytogenetics, but led to detection of a mutation in the *FLT3* gene, which is an abnormality associated with a poor prognosis in AML. This data illustrates that whole genome arrays represent a suitable tool for the detection of prognostic genomic aberrations from FFPE material in EM AML, in a clinical diagnostic setting.

2073 Tissue Identity Testing of Cancer by Short Tandem Repeat Polymorphism: Pitfalls of Interpretation in the Presence of Microsatellite Instability

MA Much, N Buza, P Hui. Yale University School of Medicine, New Haven, CT.

Background: Tissue mix-up and contamination are not infrequently encountered in the practice of surgical pathology. Tissue identity testing by analysis of short tandem repeat (STR) polymorphism offers discriminating power in resolving these problems. However, one rare but significant caveat is the presence of microsatellite instable tumors, in which genetic alterations may drastically change the STR polymorphism. This can lead to unexpected allelic discordance between the tumor and the corresponding normal tissue, and therefore erroneous interpretation. We examined how tissue identity testing can be altered by the presence of microsatellite instability (MSI) and what measures can be taken to avoid interpretation errors.

Design: Eleven cases of MSI-high (10 colorectal and 1 endometrial adenocarcinoma) and 10 cases of MSI-stable tumors (all colorectal) were selected from our pathology archives. All cases were previously tested by immunohistochemistry (IHC) for DNA mismatch repair (MMR) genes (MLH1, MSH2, MSH6 and PMS2) and by PCR using 5 NCI recommended MSI loci. DNA was extracted from microdissected tumor and normal tissues. Tissue identity testing was performed using the AmpFlSTR® Identifiler™ PCR amplification kit targeting 15 autosomal STR markers and the amelogenin locus for gender determination. The allelic patterns between tumor and normal tissue were compared in each case.

Results: Ten of 11 MSI-high tumors demonstrated novel alleles at 5 to 11 loci per case. These loci varied among MSI-high tumors, with some more frequently involved than others. However, all affected STR loci showed identifiable germline allele(s) in MSI-high tumors. One MSI-high tumor had no allelic alterations at any of the 15 STR loci, suggesting that genotyping may not detect every case of MSI. A wild-type germline allelic profile was seen in 7 of 10 MSI-stable tumors. In the remaining 3 cases isolated novel alleles were present at a unique single locus in addition to the germline alleles, likely representing the natural mutation rate of tandem repeats in microsatellites.

Conclusions: Genetic instability - particularly MSI - in tumors may significantly alter wild-type allelic polymorphism, leading to potential interpretation errors of STR genotyping. Before dismissing the tissue in question as a cancerous "floater" based on identity testing, careful examination of the allelic pattern, high index of suspicion and MSI testing by IHC and/or molecular methods are crucial to avoid erroneous conclusions and subsequent clinical and legal consequences.

2074 A Quantitative Method for Iron Histochemistry

DP Ng, LC Hyde, NB Levy, DL Ornstein. Dartmouth-Hitchcock Medical Center, Lebanon, NH.

Background: Currently, iron quantitation in histologic sections relies on discrete grades derived from manual examination of slides stained for ferric iron. In the bone marrow, several grading systems are used, ranging from a simple 3 grade score (absent/present/increased) to the more complex Gale's score with 7 grades. Several studies have suggested a high degree of interobserver variability in the application of these scoring schemes as well as inconsistency in the clinical use of these methods, suggesting a need for more reproducible and consistent methods to quantitate iron in histologic sections. Here, we report a new method to quantitate storage iron in histologic sections using open source image analysis tools.

Design: Bone marrow core biopsy sections were stained with Perl's iron and a nuclear fast red counterstain. Ten representative fields of each core were evaluated from whole slide scanned images to eliminate camera field variability. Using ImageJ, the images were separated into RGB color channels, and the red and blue channels were thresholded so that cellular (red) pixels and ferric iron (blue) pixels were selected. A ratio of number of ferric iron pixels to cellular pixels was calculated for each image and an overall average was calculated for each specimen to derive a quantitative Iron Score (qIS). Twenty sequential cores were graded by two hematopathologists using Gale's scoring system while qIS were obtained by the method above and the results compared. Interobserver variability of the field selection was analyzed with representative images from an additional 154 cores evaluated by trained and untrained independent observers for a total of 3080 images. Linear regression between qIS was performed.

Results: Using Gale's iron scoring system, the two hematopathologists showed good correlation with the log normalized qIS (R^2=0.696 and 0.663) similar to Gale's original results using radio-chemical iron analysis. Field selection by trained and untrained observers yielded excellent correlation for qIS (ρ=1.006, R^2=0.9661).

Conclusions: These results suggest that our method is useful for quantitating storage iron in bone marrow biopsy specimens and correlates well with older semi-quantitative methods. Additionally, this technique appears to be very robust and tolerant of the method by which fields are selected for analysis. This suggests that untrained observers may be trained to select fields for analysis. The use of whole slide scanning and ImageJ makes this method highly reproducible with little inter-run and inter-observer variability and can be readily applied in any lab with a camera and computer.

2075 Analytical Reproducibility of the Breast Cancer Intrinsic Subtyping Test and nCounter Analysis System Using Formalin-Fixed Paraffin-Embedded (FFPE) Breast Tumor Specimens

T Nielsen, S McDonald, S Kulkarni, J Storhoff, C Schaper, B Wallden, S Ferree, S Liu, V Hucthagowder, K Deschryver, V Holtschlag, G Barry, M Evenson, N Dowidar, M Maysuria, D Gao. British Columbia Cancer Agency, Vancouver, BC, Canada; Washington University School of Medicine, St. Louis, MO; NanoString Technologies, Seattle, WA; MyRAQA Inc., Redwood Shores, CA.

Background: NanoString's breast cancer intrinsic subtyping test is based on the previously reported PAM50 gene expression signature. The test is performed on the nCounter Analysis System using gene-specific fluorescently labeled probe pairs that hybridize directly to target mRNAs in solution. The intrinsic subtype (Luminal A/B, Her2-enriched, Basal-like), ROR score (0-100 scale), and risk category are determined by the system using a prospectively defined and locked algorithm. A recent clinical validation in over 1000 patient specimens from the ATAC trial demonstrated that the ROR score added significant prognostic information beyond the Oncotype DX® RS score in estimating the likelihood of distant recurrence in hormone receptor positive, post-menopausal breast cancer patients. The validation studies described here were designed to measure the analytical robustness of the test across three clinical testing sites.

Design: Analytical precision was measured by testing five pooled breast tumor RNA samples representing each breast cancer subtype and risk classification group across three sites, six operators, and three reagent lots. Each site completed 18 valid runs consisting of 10 tests each. Reproducibility was measured by testing replicate tissue sections from 43 FFPE breast tumor blocks following independent review of an H&E stained slide by a pathologist at each site to mark the area of invasive carcinoma. Following macrodissection of tumor tissue, total RNA was isolated and 125 – 500 ng RNA was tested on the nCounter system.

Results: Within each RNA sample, the measured SD was less than 1 ROR unit including all sources of variation, and there were no significant differences in performance by operator or site. In the reproducibility study, the measured total SD of the ROR score across all samples was 2.9 ROR units. The average site to site concordance of risk category was > 90 %, and there were no low-to-high risk mis-classifications (or vice versa). The average site to site subtype call concordance was 97 %.

Conclusions: The nCounter system provides a highly precise method for measuring clinically-relevant gene expression signatures on FFPE surgical pathology specimens, and the analytical reproducibility of the test has been validated using FFPE breast tumor specimens across multiple clinical testing laboratories.

2076 Optimum Number of H&E Levels in the Workup of Bronchial Biopsies

J Nunez, JF Silverman, U Krishnamurti. Allegheny General Hospital, Pittsburgh, PA.

Background: Transbronchial biopsies are often used in the initial work up of lung lesions providing important information for diagnosis, treatment and prognosis. In addition to evaluation of H& E sections, there is a growing need to conserve tissue for ancillary studies such as immunohistochemistry, molecular studies and occasionally histochemistry. The optimum number of H&E levels for evaluation has not been clearly established. In the past, 5 H&E levels were performed at our institution. However, recently we obtained three levels with the intent of conserving tissue for potentially needed ancillary studies. The aim of this study was to determine the optimal number of H& E levels for diagnosis of bronchial biopsies to allow conservation of tissue for additional ancillary studies.

Design: A total of 52 cases of bronchial biopsies were retrieved from the pathology data base (01/2004 to 04/2012), with 45 cases having 5 levels and 7 cases having only 3 levels. There were 20 cases of non-small cell lung carcinoma, 9 cases of small cell lung carcinoma and 24 cases of granulomatous and infectious processes. The slides were reviewed by two investigators, and an evaluation of the amount of diagnostic material in each H&E level was recorded.

Results: Adequate diagnostic material was found in 50/52 (96%) cases in level 1, 52/52 (100%) cases in level 2, 52/52 (100%) in level 3, 40/45 (88%) cases in level 4 and 36/45 (80%) cases in level 5. Therefore, limited amount of diagnostic material was present in levels 1, 4 and 5 in 4%, 12% and 20% of cases respectively. The maximum amount of diagnostic material was seen in levels 2 and 3 in 100% of cases.

Conclusions: Our study demonstrates that it is optimal to initially obtain only 3 H&E levels in bronchial biopsies, in order to conserve tissue for potential ancillary studies. In cases with no diagnostic material present initially in the first 3 levels, additional levels can then be obtained. In our laboratory, we are currently obtaining 3 H&E levels for initial evaluation of bronchial biopsies without any compromise of diagnostic material.

2077 Lack of Reactivity with TdT in Small Cell Carcinoma

BR Oliai, CJ Buresh, RT Miller. ProPath Laboratory, Dallas, TX.

Background: The differential diagnosis between small cell carcinoma (SCC) and Merkel cell carcinoma (MCC) can be difficult as both are high grade neuroendocrine carcinomas which share many cytomorphologic and immunophenotypic features. Previous reports have shown that significant expression of TdT can be seen in up to 73% of MCC. Thus far we are aware of only one published report examining the expression of TdT in a series of 30 SCC. Herein we report our experience with TdT expression in a series of 108 cases of SCC.

Design: We reviewed 108 cases of SCC sent to our group in consultation for confirmatory immunophenotyping over a 5 year period. All tumors demonstrated the typical perinuclear dotlike staining pattern with low molecular weight cytokeratin. All but 2 cases expressed a combination of the neuroendocrine markers CD56, synaptophysin, and chromogranin (1 case expressed only CD56 and 1 case only synaptophysin). All but 4 cases expressed strong diffuse nuclear TTF-1 immunoreactivity (with 2 negative cases and 2 cases showing only focal staining of 5% or less cells). All cases demonstrated very high proliferation rates, as assessed by Ki-67 immunostaining. Cytokeratin 20 immunostaining was performed in 83 cases, with only 6 cases demonstrating reactivity (5 cases showing focal, dim staining and 1 case showing diffuse perinuclear dotlike staining), all positive cases demonstrated strong, diffuse nuclear TTF-1 reactivity.

Results: Of 108 cases of SCC, only 3 (2.7%) demonstrated reactivity with TdT, with only 5-15% of cells staining.

Conclusions: Since previous work has shown that TdT is positive in up to 73% of MCC, TdT may well be a useful immunostain in the differential diagnosis between SCC and MCC, with negative staining arguing in favor of SCC.

2078 Urine Biobanking: Methods, Validation, and Research Results

JL Owens, JM DiPiero, P Elson, DE Hansel. Cleveland Clinic, Cleveland, OH.

Background: Bladder cancer is a significant cause of morbidity and mortality worldwide, and is difficult to detect early in disease progression, having few obvious symptoms aside from hematuria. An early urine-based diagnostic marker for low and high grade bladder cancer would be of significant value in early detection and treatment of bladder cancer.

Design: Whole urine, and centrifuged urine supernatant and cell pellets were each banked from catheterized samples taken from >200 patients being monitored for bladder cancer. Patients were stratified into groups who showed either no signs of disease, low grade bladder cancer, or high grade bladder cancer. All patient groups were confirmed by cystoscopic observations, and the latter groups were confirmed by biopsy and histopathological examination. Quantities of free RNA and DNA were compared across each urine product for 155 patients, 34 in the non-disease group, 51 in the low grade group, and 70 in the high grade group. RNA was extracted from 24 patient cell pellets; eight from non-diseased patients, eight from patients with low grade bladder cancer, and eight from patients with high grade bladder cancer. Microarray analysis and PCR validation were performed on each RNA sample, and the microarray data was analyzed for genes that were differentially expressed between patients with no disease and all patients with bladder cancer, as well as genes that were differentially expressed between patients with low grade bladder cancer and high grade bladder cancer.

Results: The cell pellet was confirmed to be the most efficient method of biobanking urine if the goal is RNA or DNA extraction. Several genes of interest were identified in the microarray analysis for possible future use as diagnostic or prognostic biomarkers.

Conclusions: Urine is a high-priority body fluid for banking, and the methods described result in excellent nucleic acid preservation. Urine-based biomarker assays for bladder cancer are a valuable addition to a care provider's arsenal for early discovery of bladder cancer.

2079 Intraoperative Pathologic Consulation by Telepathology: An Accuracy Study of 104 Analysis Performed by the Eastern Quebec Telepathology Network

E Perron, B Tetu. CHUQ-Hotel-Dieu de Quebec, Quebec, QC, Canada; Centre Hospitalier de Baie-Comeau, Baie-Comeau, QC, Canada; Faculty of Medicine, Université Laval, Quebec, QC, Canada.

Background: In 2004, Quebec ministry of health and Canada Health Infoway supported the creation of the "Eastern Quebec Telepathology Network" aimed at providing uniform diagnostic telepathology services in a huge territory (408,760 km^2 and 24 hospitals). The objective of this study is to evaluate the accuracy of the first frozen sections performed by telepathology and to assess the time required to perform the analysis.

Design: We performed a retrospective review of the first 104 consecutive intraoperative frozen sections evaluated by telepathology. The real-time gross evaluation was performed using a macroscopy station (PathStand 40, Diagnostic Instruments, *Sterling Height, USA*) and two videoconferencing devices (PCS-XG80DS Codec, Sony, *Minato, Tokyo, Japan*). Those equipments were obtained from Olympus Canada.Inc (*Markham*, Canada). The slides were scanned at a 20X magnification on a Nanozoomer 2.0 HT (Hamamatsu Photonics, *Shizuoka Prefecture, Japan*). The visualisation was at a 1680 x 1050 pixels resolution with the mScope v.3.6.1 (Aurora Interactive Ltd., *Montreal, Canada*) software. The diagnosis given to the surgeon and documented in the intraoperative pathology report was compared with the final pathology report. In the cases of a discrepancy, the frozen section slides, the paraffin slides and the scanned slides were reviewed to determine the reason for the error.

Results: Of the 104 cases, 102 cases were either concordant or with no clinically significant discrepancies (8 diagnoses were slightly discrepant because of differences in terminology in the same category of interpretation). Therefore, the percentage of agreement was 98%. Two significant discordant cases were reported: a change from a negative margin to a low grade intraepithelial lesion and the finding of a micrometastase in a lymph node. The average time from the arrival of the specimen to the intraoperative diagnosis was 20 minutes and it took an average of 8 minutes once the frozen section slide was ready until the diagnosis.

Conclusions: The Eastern Quebec Telepathology Network allowed to maintain a quality intraoperative frozen section service in a hospital where no pathologist was available on site. Telepathology allows greater flexibility in practice, avoids unnecessary travel and facilitates a better organisation of work in a vast territory with a shortage of pathologists.

2080 Image Analysis of Ki-67 IHC Stain for Breast Carcinoma – A Study Comparing Two Image Analysis Systems

AM Plagge, T Mounajjed, JS Voss, DM Minot, DJ Tuve, BR Kipp. Mayo Clinic, Rochester, MN.

Background: Ki-67 immunohistochemisty (IHC) is often used to evaluate the proliferative activity of paraffin-embedded breast cancer and may provide useful prognostic information. The goal of this study was to evaluate the reproducibility and analysis time of different digital Ki-67 scoring methodologies on breast carcinoma specimens.

Design: Ten cases containing invasive or metastatic breast carcinoma from specimens previously analyzed clinically for Ki-67 IHC were selected for this study. The slides were scanned with our current analysis method using the Dako ACIS III (Automated Cellular Imaging System) and the Aperio ScanScope instrument to create digital images. The images were independently analyzed by three Cytotechnologists using three different scoring methods. ACIS analysis was performed by selecting 8-10, 40X sized fields of view representative of the overall staining within the tumor. The specimens analyzed using Aperio software were circled to encompass at least 75-100% of the invasive tumor by two methods: 1)a Wacom Cintiq 21UX tablet monitor (21.3 inch screen) with an interactive pen (tablet tracing) and 2)a standard 19 inch computer monitor with mouse (mouse tracing). All analyses were timed with results recorded.

Results: Data analysis revealed that the three Ki-67 quantitation methods produced very similar results. Ki-67 scores obtained by both Aperio tumor tracing methods correlated with those obtained by the ACIS method, with R^2 values of 0.934 and 0.930 for the mouse and tablet tracing methods, respectively. The mouse and tablet tracing methods also had excellent correlation of Ki-67 scores (R^2=0.993). While the three scoring methods produced similar Ki-67 results, the two Aperio tumor tracing methods tended to produce more consistent Ki-67 scores for each case by different technologists (SD=2.88 and 1.93 for tablet and mouse methods) than the ACIS method (SD=5.75). However, the average analysis time per case was lowest using the ACIS instrument (3 min, 8 sec) compared to 11 minutes, 23 seconds for the mouse tracing method and 10 minutes, 26 seconds for the tablet tracing method.

Conclusions: While Ki-67 quantitation using the ACIS instrument can be performed considerably quicker than the Aperio tumor tracing methods, it is not as reproducible as the Aperio tracing methods. Aperio analysis using a tablet monitor and pen reduces analysis time when compared to a standard computer monitor and mouse. Further studies are needed to find ways to reduce Aperio analysis time while maintaining the high reproducibility of tumor tracing techniques.

2081 Quantitative Assessment of Mutant Allele Burden in Solid Tumors by Semiconductor Based Multi-Gene Next Generation Sequencing

BP Portier, R Luthra, R Singh, M Routbort, B Handal, N Reddy, BA Barkoh, Z Zuo, LJ Medeiros, K Aldape, KP Patel. MD Anderson, Houston, TX.

Background: The ability of next generation sequencing (NGS) to provide a quantitative assessment of mutant allele burden in multiple genes provides a significant advantage over conventional qualitative genotyping platforms such as Sanger sequencing or quantitative platforms with limited multiplexing capabilities. Quantitative assessments of mutatant allele burden are likely to yield significant insights into tumor biology

with regards to tumor heterogeneity and clonal evolution. In this study, we assessed the quantitative ability of semiconductor based NGS to that of an alternate quantitative platform and determined correlation with morphologic assessment of tumor percentage.
Design: DNA was isolated from 45 microdissected, formalin fixed paraffin embedded solid tumors with a somatic mutation detected by a quantitative primer-extension MALDI-TOF assay (PE-MALDI). Tumor percentages ranged from 20-95% as verified by pathologist consensus. The PE-MALDI assay interrogated hotspot mutations in 11-genes. NGS was performed utilizing the 46-gene Ion AmpliSeq™ Cancer Panel (Life Technologies, CA, USA). Mutant allele burden was calculated as a ratio of mutant allele to combined mutant and wild type alleles. Mutant allele burden in *BRAF, KRAS, MET* and *NRAS* were used for the correlation study. Statistical analysis was performed using GraphPad Prism 6.0.
Results: NGS-based estimation of mutant allele burden ranged from 13.6% to 79.1% for all 45 solid tumor samples (Individual genes: *BRAF* (13.6-79.1%), *KRAS* (14.1-66.5%), *NRAS* (15.1-78.1%), and *MET* (46.1-57.7%)). NGS detected all mutant alleles identified by PE-MALDI (100% concordance). The correlation between NGS and PE-MALDI for all interrogated mutations was r^2= 0.85 (P< 0.0001). The correlation between NGS and PE-MALDI for individual genes was BRAF r^2= 0.90, KRAS r^2= 0.94, and NRAS r^2= 0.92 (P< 0.0001). Correlation for *MET* (n=6) did not reach statistical significance r^2= 0.60 (P= 0.071). Pathologist based morphologic assessment of tumor percentage did not correlate to the percent mutant alleles detected by either NGS (P=0.20) or PE-MALDI (P=0.61).
Conclusions: NGS-based multi-gene sequencing using nanogram amounts of DNA allows quantitative assessment of mutant allele burden, comparable to lower throughput quantitative mutation analysis platforms. The ability to use high-throughput NGS to quantitatively measure somatic mutations in solid tumors will rapidly advance our basic knowledge of tumor biology and ultimately will advance our ability to offer personalized cancer care.

2082 Analysis of Common Chromosomal Abnormalities in Hematopoietic Stem Cells by FISH in Multiple Myeloma for Determination of Early Lineage Involvement

F Saei Hamedani, J Lopategui, R Pillai, K Baden, RA Vescio, S Alkan. Cedars-Sinai Medical Center, Los Angeles, CA.
Background: Multiple myeloma (MM) is characterized by a clonal expansion of malignant plasma cells that usually show certain cytogenetic abnormalities such as 13q del, t (11; 14), 17p del. Patients treated with autologous bone marrow transplantation eventually relapse that raise a question whether MM is a hematopoietic stem cell disorder. In order to investigate whether hematopoietic stem cells have the same cytogenetic abnormalities as the neoplastic plasma cells, we have developed a novel method to assess presence of MM associated cytogenetic abnormalities utilizing magnetically separated CD34+ hematopoietic cells.
Design: Bone marrow aspirates from patients with clinical suspicion of MM were analyzed by standard cytogenetic studies. In addition, MM samples were subject to FISH analysis using probes specific for commonly encountered cytogenetic abnormalities in MM. Mononuclear cells from bone marrow aspirate were separated using Ficoll-Paque. CD34+ cells were separated from mononuclear cells with EasySep® Human CD34+ Positive Selection Kit from Stem Cell Technologies (Vancouver, Canada). Isolated CD34+ cells were assessed for purity with flow cytometric analysis using antibodies against CD34, CD38, CD138, and CD45. Cytospin samples following CD34 selection were prepared to microscopically assess the morphology of the isolated cells that were subjected to FISH analysis using probes against the specific abnormalities detected by cytogenetic/FISH studies in the corresponding non-purified plasma cells.
Results: Magnetically separated samples yielded 1-2% CD34+ cells after selection by CD34-antibody coated beads. Common cytogenetic abnormalities were noted in unfractionated MM samples using FISH analysis in the bone marrow aspirates. Flow cytometric analysis revealed that purity of the magnetically separated CD34+ cells was more than 90%. The CD34-enriched cell population subjected to FISH assay did not show any abnormalities that were detected in plasma cells.
Conclusions: The lack of cytogenetic abnormalities in CD34+ stem cell population indicates that the chromosomal abnormalities detected in plasma cells are likely to occur in the later stages of B-cell development. Our results suggest that the hematopoietic stem cells (CD34+ cells) do not have the same chromosomal abnormalities noted in the plasma cells in MM patients. Therefore, failure in MM patients treated with autologous bone marrow transplantation is most likely due to the growth of the chemotherapy-resistant cells residing in the host.

2083 Useful Immunohistochemical Technique in Heavily Pigmented Malignant Melanoma

M Shimizu, Y Hosonuma, H Yamaguchi, K Nagata, M Yasuda. Saitama Medical University International Medical Center, Hidaka, Saitama, Japan.
Background: Immunohistochemistry is often used in the diagnosis of malignant melanoma. However, evaluation can be challenging in heavily pigmented cases because immunohistochemical staining for HMB-45 and Melan-A antibodies using diaminobenzidine (DAB) as the chromogen reveals a brown product, which cannot distinguish melanocytes from melanophages. In such cases, alkaline phosphatase-fast red detection method may be conducted in some institutions. Here, we specifically paid attention to the process of counterstaining in immunohistochemistry.
Design: Fifteen examples of heavily pigmented malignant melanoma were immunohistochemically evaluated by using HMB-45, Melan-A, and microphthalmia transcription factor (MiTF). Immunohistochemistry was performed using four different stains, Giemsa stain, methylene blue stain, toluidine blue stain and cresyl violet stain, as counterstains, and then these four counterstains were compared with one another in terms of their staining quality, handling time, facility and cost.
Results: Thirty minutes was the appropriate time to obtain adequate metachromasia in melanin pigment. All four counterstains showed melanin and melanophages as green blue staining, which can easily contrast with DAB, regardless of the antibody tested. On the other hand, positive melanoma cells showed as brown in most cases. Among the four counter stains described above, methylene blue stain was the most useful because of its better staining quality, shorter handling time and easier handling. Regarding the immersion time, methylene blue stain was only three minutes and was shorter than the other stains (10 to 30 minutes). In areas that were difficult to evaluate immunohistochemically, the addition of immunohistochemical staining using MIB-1 and CD68 was found to be useful.
Conclusions: Modified immunohistochemical technique by counterstain with methylene blue is the most useful diagnostic tool in evaluating heavily pigmented malignant melanoma. It should be performed when encountering heavily pigmented melanocytic lesions, not only melanoma but also blue nevi, pigmented epithelioidmelanocytoma, and pigmented spindle cell variant of Spitz nevi.

2084 Role of Magnification in Visual Evaluation of Manual and Automated HPV In-Situ Hybridization in Oropharyngeal Carcinoma Biopsy Samples

MT Siddiqui, C Cohen, N Fatima. Emory University Hospital, Atlanta, GA.
Background: Determination of Human papillomavirus (HPV) status has strong diagnostic, prognostic, and therapeutic implications in oropharyngeal cancers (OC). Determining the integration status of HPV by in situ hybridization (ISH) is cost effective and routinely utilized in clinical practice. However, the reliability of reporting is dependent on individual expertise and visual evaluation. In this study, we have compared the role of magnification in interpreting HPV ISH results of manual versus an automated method, using the Dako and the Enzo probe respectively.
Design: We evaluated 55 small biopsies of primary OC utilizing HPV ISH manual with the Dako probe and Leica Bond-III automation using the Enzo probe. Punctate dot-like nuclear positivity observed with low, intermediate or high magnifications, 10 x, 20 x or 40-60x, was assigned as 3+, 2+ and 1+ respectively. A single cell showing nuclear punctate dot-like staining was considered a positive result.
Results: Ten of 55 (18%) biopsies with manual HPV ISH and 30 of 55 (54%) biopsies with the automation method positive at 10x magnification, were considered 3+. Twenty two of 55 (40%) biopsies with manual HPV ISH and 6 of 55 (10%) biopsies with automation positive at 20x magnification, were 2+. Seven of 55 (12%) biopsies with manual HPV ISH and 14 of 55 (25%) biopsies with automation positive at 40-60x magnification, were considered 1+.

([table1])

HPV ISH (Positive)	10X (3+)	20X (2+)	40-60X (1+)
Manual	10/55 (18%)	22/55 (40%)	7/55 (12%)
Automated	30/55 (54%)	6/55 (10%)	14/55 (25%)

Conclusions: Magnification power plays a critical role in visual evaluation of HPV ISH. The dot like punctate staining may be very focal which requires careful visual determination of all tumor cells. Low magnification (10x) reveals positivity in 18% of cases with the manual method, whereas the automated technique, being more sensitive, reveals a high positivity rate (54%). Hence, automation provides a better and more efficient method for evaluating HPV ISH. Failure to evaluate under high magnification (40-60x) however, could give false negative results in 12% of cases with the manual method and 25% with automation. This could confound the analysis and effect therapeutic decisions.

2085 Detection of Her2/Neu Overexpression in Gastric Adenocarcinmas Using the Novel RNAScope Method

AD Singhi, Y Luo, H Wang, X-J Ma, PB Illei. University of Pittsburgh, Pittsburgh, PA; Advanced Cell Diagnostics, Inc, Hayward, CA; Johns Hopkins University, Baltimore, MD.
Background: Approximately 20% of gastric adenocarcinomas are Her2 positive and may benefit from trastuzumab therapy. In gastric carcinoma Her2 protein expression and gene amplification dos not correlate as well as in breast carcinomas and therefore the use of more than one method is recommended. Her2 protein expression is strongly influenced by pre-analytical factors leading to false negative results. A robust RNA in-situ hybridization (ISH) assay using FFPE could represent an alternative method for accurately evaluating Her2/neu expression.
Design: Tissue microarrays of 55 cases of gastric adenocarcinomas were subjected to the RNAScope Her2 in situ hybridization method (Advanced Cell Diagnostics, Inc., Hayward, CA) and a previously established scoring method. Matching slides were also subjected to Her2 immunohistochemistry using Herceptest (Dako, Carpintera, CA) and the 4B5 monoclonal antibody (Ventana Medical Systems, Tucson, AZ) using standardized FDA approved protocols and scoring guidelines.
Results: Tumors were from 22 female and 33 male patients (28-81 years; mean 62.2 years). HER2 mRNA molecules were detected as punctate dots. Samples with >15 HER2 mRNA dots/cell were classified as positive. Seven tumors were positive by RNA ISH and 6 of them were positive by both IHC assay. RNA positive tumor was positive (3+) using the 4B5 antibody and equivocal (2+) using Herceptest. This case showed an average of 10 signal dots in 100% of the tumor cells. One more tumor showed similar RNA signaling (10 signals in 100% of tumor cells) and was negative by both immunohistochemistry method (score 0). One RNA ISH positive tumor was negative by Herceptest and one 4B5 positive tumor was negative by RNA ISH. All other cases were negative by all 3 assays.
Conclusions: Her2/neu protein expression evaluated by immunohistochemistry correlated well with increased Her2/neu RNA levels as assessed by the RNAScope RNA ISH method. The signals are crisp and are easy to read. Since the signal detection utilizes a chromogenic detection the signals can be localized to tumor cells (including high grade

dysplasia). In contrast, this can be difficult to perform when using fluorescent in situ hybridization (FISH) especially in small biopsy samples where a large number of non-neoplastic cells can be present. Furthermore, the recent release of an automated method for performing the RNAScope assay (Ventana Discovery) has made the hybridization easier to perform and more reproducible.

2086 A Simple and Cost-Effective Method of DNA Extraction from Small Formalin-Fixed Paraffin-Embedded Tissue for Molecular Oncology Testing: A Practical Approach

AN Snow, AA Stence, JA Pruessner, S Forde, S Edler, AD Bossler, D Ma. University of Iowa Hospitals and Clinics, Iowa City, IA.

Background: Extraction of DNA from formalin-fixed, paraffin-embedded (FFPE) tissue is a critical step in molecular oncology testing. This is particularly challenging with tiny biopsies with limited tumor cells in a background of non-tumor cells. It is cost prohibitive for many laboratories to invest in laser capture microdissection. We compared our standard procedure of manually scraping tissue from unstained slides with a glue capture method (Pinpoint Solution, Zymo Research Corp, Inc) on H&E stained slides and optimized the DNA extraction protocol.

Design: FFPE tissue blocks were selected from previously tested cases from our laboratory. Areas with tumor ranging from 1-2 mm^2 were marked by a pathologist. Sections were either scraped with a razor blade or deparaffinized and H&E stained for tumor cell capture using the Pinpoint solution. Tissue bound to the solution was microdissected, and genomic DNA was isolated according to the manufacturer's instructions for the Pinpoint Slide DNA Isolation or QIAamp DNA FFPE Tissue kit (Qiagen, Inc.).

Results: DNA yield was 10-fold higher using the QIAamp method compared with the Pinpoint method when following the manufacturer's recommendation of a 4 hour proteinase K (PK) digestion. Although longer incubation with PK increased the DNA yield from this method, it was still about 60 ng/mm^2 less than with the QIAamp method. Mutations detected included BRAF V600E in melanoma by primer extension, a 15 base pair deletion and a SNP in the EGFR gene from a transbronchial lung biopsy using Sanger sequencing, G12D and G12C mutations in KRAS from colon biopsies by primer extension, and a multiplex PCR-based assay for microsatellite instability from a colon biopsy with clusters of signet ring cells in pools of mucin. DNA from both kits gave equivalent results on all molecular tests performed. When significantly less DNA (about 90% decrease on average) was used, the test performance was not affected in comparison with the original testing. Cost analysis revealed a savings of 24.4% with the new procedure.

Conclusions: Using H&E stained slides allows visual confirmation of tumor cells during microdissection. The Pinpoint solution made removal of tissue from the slides easier. Blending the two kits increased yield and reduced cost. Valid test results were obtained across multiple molecular oncologic testing platforms with 90% less tissue and 70.9% to 93.6% less DNA. This DNA extraction method is simple, cost-effective, and blends with our current workflow requiring no additional equipment.

2087 SLIM: *Tool To Aid Pathologists in Separation of Prostate Cancer Gleason Grade 3 and 4*

S Sridharan, J Liang, A Marar, L Wang, K Shah, R Tapping, V Macias, K Tangella, A Kajdacsy-Balla, G Popescu. University of Illinois at Urbana-Champaign, Urbana, IL; University of Illinois at Chicago, Chicago, IL; Christie Clinic, Urbana, IL.

Background: Spatial Light Interference Microscopy (SLIM) is an add-on module to the commercial phase microscope which enables us to obtain a refractive index map of an unstained, transparent sample of constant thickness. In the past SLIM has been used to diagnose prostate cancer, and now we propose to use it to help in separation of Gleason grade 3 vs. Gleason 4.

Design: Prostate tissue microarray (TMA) with cores of different Gleason grades was obtained from the CPCTR collection. Twenty-two unstained cores with Gleason grade 3 and 21 unstained cores with Gleason grade 4 prostate cancer were imaged using SLIM at 40X/0.75NA. We measured the solidity of 6-8 glands per core (patient), which is the ratio of the area occupied by the glands to the area of an elliptical fit for the gland. We also measured the anisotropy of stroma adjoining each of these glands, which is the square of the ratio of the phase gradient to the phase variance.

Results: Our results indicate that Gleason grade 3 glands have higher glandular solidity and lower anisotropy in stroma adjoining the gland compared to glands of Gleason grade 4. By creating a scatter plot of glandular solidity vs. stroma anisotropy for each gland in an image, we can separate Gleason grade 3 from Gleason grade 4 and therefore determine Gleason scores in a given image. Thirty- four cores out of 43 were correctly classified by SLIM (79%).

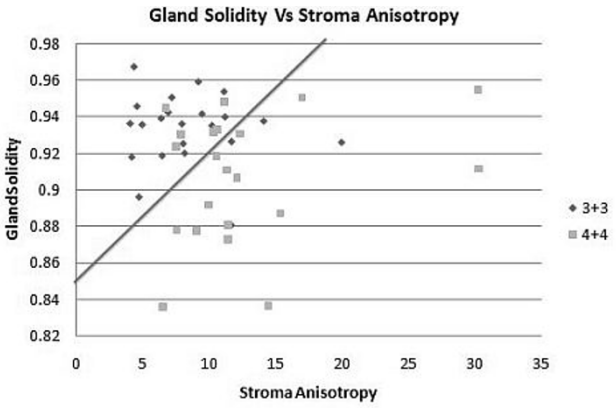

Conclusions: SLIM can be a valuable tool in aiding pathologists in Gleason grading of prostate cancer. Further work needs to be done to automate the process.

2088 Comparison of LMP-1 Immunostaining Patterns with EBER-ISH Reactivity

J Thomas. Louisiana State University Health Science Center, Shreveport, LA.

Background: Detection of Epstein-Barr virus (EBV) in tissue may be achieved by various methods including EBV-encoded RNA (EBER) in-situ hybridization (ISH) and immunohistochemistry (IHC) for latent membrane protein (LMP-1). EBER-ISH is recommended as the best test for detecting and localizing latent EBV in tissue samples, however, manual IHC is more readily available in low-resource settings. Though membrane and/or cytoplasmic dot-like staining of IHC for LMP-1 is interpreted as positive, diffuse and granular cytoplasmic reactivity are sometimes seen and interpretation of these is uncertain. The IHC LMP-1 and EBER-ISH reaction in nasopharyngeal carcinomas (NPC) are compared to determine the reliability of these reactions.

Design: All NPC identified over a 4-year period in the Pathology database of UCH, Ibadan were retrieved and reviewed. IHC for LMP-1 and EBER-ISH were performed. Both staining reactivity was compared to determine the diagnostic accuracy of IHC. RNA and negative controls were performed.

Results: 32 cases of NPC were identified; 18 LMP-1 IHC are negative and 8 cases are considered positive with membrane and cytoplasmic staining, including 5 cases with dot-like, Golgi pattern. Equivocal LMP-1 IHC diffuse or granular cytoplasmic staining are present in 6 cases all are EBER-ISH positive.

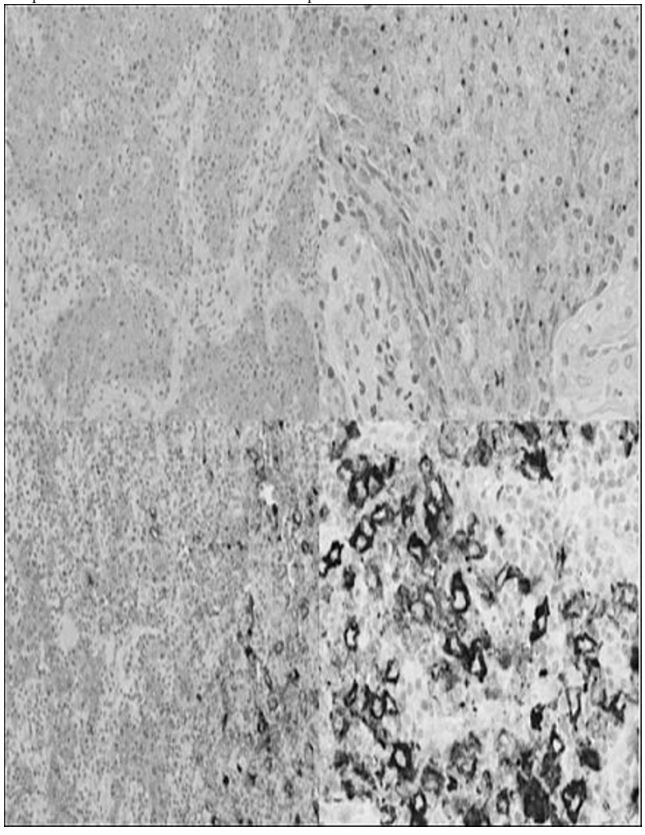

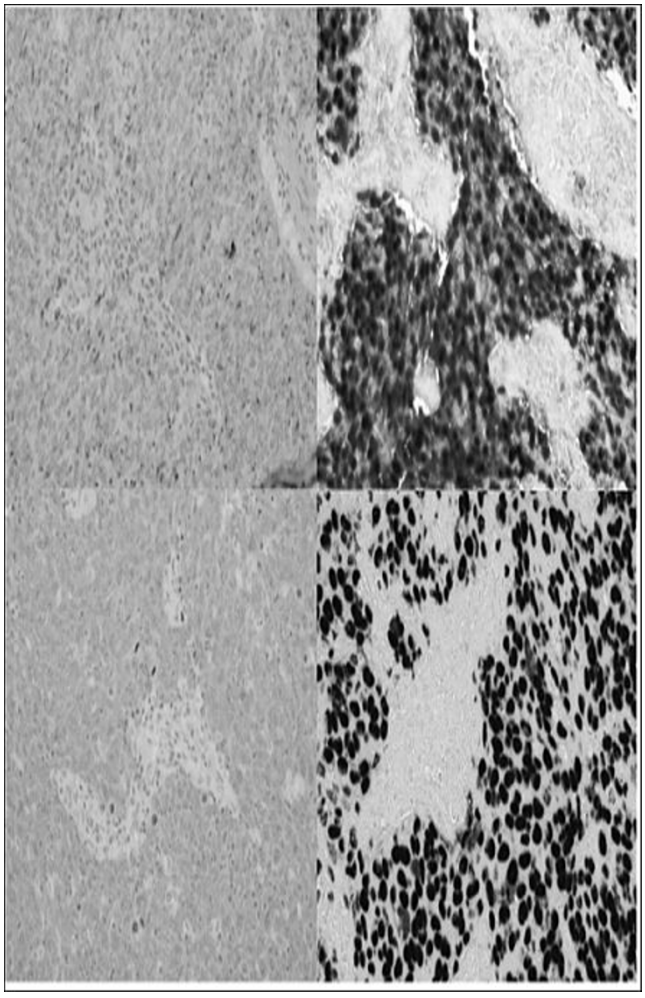

12 cases showed discordant reaction; all are LMP-1 IHC negative, EBER-ISH positive. EBER-ISH signal is localized to the nuclei.

Conclusions: LMP-1 IHC is more economical, rapid and easily incorporated into routine laboratory compared to EBER-ISH. Diffuse, granular and dot-like Golgi cytoplasmic LMP-1 IHC reactvity should be considered positive at least, in NPC.

2089 Metabolites and Histology on Exactly the Same Biopsy Tissue

DA Troyer, JR Shuster, R Lance. Eastern Virginia Medical School, Norfolk, VA; Biomarker Factory, Durham, NC.

Background: An increasing number of molecular biomarker assays are performed that frequently compete with histopathology for the same tissue. Small molecule metabolites are increasingly recognized as potential biomarkers of cancer and other diseases. We have developed a method to assay metabolites and perform histology on the exact same tissue called molecular preservation by extraction and fixation (mPREF).

Design: 18 gauge core-needle biopsies taken *ex vivo* from human prostatectomy samples were immediately placed in 1 mL of 80% aqueous methanol. After 12-24 hours, biopsy cores were transferred to formalin and processed by standard histologic methods. The methanol is retained for metabolite analysis. From more than 200 small molecules identified on a metabolomics platform, we have selected nine for quantification by liquid chromatography/mass spectroscopy (LC/MS): betaine, malate, proline, N-acetylaspartate, uracil, xanthine, cysteine, and alanine. The molecules were chosen in part because their physical and chemical properties allows them to be run on a single LC/MS run.

Results: Preliminary results showed trends in tumor *vs.* no tumor for betaine, proline, uracil, cysteine, and N-acetylglucosamine when normalized to the biopsy surface area. Shown in the attached table are results for a total of 15 normal/tumor pairs.

Metabolite Quantitation

Metabolite	No Tumor µM/cm2	Tumor µM/cm2
betaine	2.04	4.71
malate	30.23	33.92
proline	42.94	47.54
N-acetylaspartate	2.79	2.99
uracil	41.13	50.56
xanthine	3.90	4.38
cysteine	877.90	1209.76
alanine	948.75	927.44
N-acetylglucosamine	20.86	28.97

Legend: µM/Cm2 = data normalized to surface area of the biopsy core

Histopathology using routinely processed paraffin embedded tissue following methanol treatment was satisfactory. IHC for basal keratin and p63 also performed well.

Conclusions: The results indicated that quantitation of metabolite molecules is feasible in 18 gauge core needle biopsies of prostate tissue. Studies are underway to determine the best means of normalizing metabolite results to overall size of individual biopsies and to volumes of tumor, non-tumor stroma, and normal glands. mPREF aligns well with existing histology workflows as the tissue is moved from alcohol to formalin. Once immersed in formalin, the tissue can be processed by any histology laboratory. The literature indicates that alcohol fixed tissues are suitable for FISH, IHC, and for extraction of RNA and DNA.

2090 Acid Hematoxylin Is an Alternative to Feulgen Staining for Cytology Specimens and DNA Ploidy Analysis

N Valkov, R Voyles, M Kulikowski, D Hossain, DG Bostwick. Bostwick Laboratories, Inc., Orlando, FL.

Background: Feulgen stain is the standard for nuclear image analysis and DNA ploidy analysis, but is laborious, expensive, and difficult to successfully employ with cytologic specimens owing to variable staining and loss of cells during the acid hydrolysis stage. In this report, we evaluated the utility of a potential alternative- acid hematoxylin- to Feulgen stain for cytology and DNA ploidy analysis.

Design: We undertook a split-sample comparative analysis of endometrial brush cytology samples and random void urine cytology specimens stained with Feulgen and acid hematoxylin. Brightfield digital images were analyzed for staining intensity and DNA ploidy analysis.

Results: Cell yield was invariably greater with acid hematoxylin than Feulgen stain, especially in urine samples. DNA ploidy analyses were remarkably similar, with Pearson's correlation coefficients (r) of 0.96 and 0.99 for endometrial and urine cytology specimens, respectively.

Conclusions: Acid hematoxylin had similar performance characteristics as Feulgen in DNA determination of ploidy, but was technically easier and considerably less expensive with greater cell yield for both sets of specimens.

2091 Improved Detection of Diffuse Large B-Cell Lymphoma by Flow Cytometric Immunophenotyping – Effect of Tissue Disaggregation Method

BD Vallangeon, C Tyer, A Lagoo. Duke University Medical Center, Durham, NC.

Background: Flow cytometric immunophenotyping is recognized as a rapid, sensitive and accurate method for diagnosis of B-cell lymphomas. We observed that flow cytometry failed to identify the clonal B-cell population in several cases of large B-cell lymphoma (DLBCL) when tissue samples were prepared by a commercially available mechanical tissue disaggregation method. To overcome this shortcoming, we tested a manual tissue disaggregation method and compared it with the mechanical method.

Design: Flow cytometry findings from 51 cases of DLBCL processed with the mechanical tissue disaggregation method, 27 cases processed using the manual method and 15 cases processed using a combination of both methods were compared. The results of the morphologic examination and immunohistochemical stains in each case were reviewed.

Results: Flow cytometry detected a clonal B-cell population in 88.9% (24/27) of cases processed by the manual tissue disaggregation method, but only in 66.7% (10/15) of cases processed by a combination of the manual and mechanical disaggregation methods, and in 62.7% (32/51) of cases processed solely by the mechanical tissue disaggregation method ($p < 0.01$ Fisher exact). Among the cases which were negative by flow cytometry, necrosis was noted microscopically in 66.7% (2/3) of those processed manually compared to 42.1% (8/19) of those processed mechanically. Manual processing yielded positive flow cytometry results in 81.8% (9/11) of the nodal tissue samples and 93.8% (15/16) of the extra-nodal tissue samples, whereas mechanical disaggregation was particularly inefficient in preserving large lymphoma cells from extranodal tissue: 71.4% (10/14) of the nodal tissue samples and 56.8% (21/37) of the extra-nodal tissue samples processed by the mechanical method showed clonal B-cells by flow cytometry ($p < 0.006$, Fisher exact).

Conclusions: The diagnostic yield of flow cytometry in diffuse large B-cell lymphoma can be significantly improved by utilizing a manual disaggregation method, particularly in extra nodal tissue samples.

2092 Label-Free High-Resolution Infrared Spectroscopic Imaging for Breast Tissue Histopathology

MJ Walsh, S Biswas, A Kajdacsy-Balla, R Bhargava. University of Illinois at Urbana-Champaign, Urbana, IL; University of Illinois at Chicago, Chicago, IL.

Background: Histopathology forms for the gold standard for breast cancer diagnosis. Current methodologies require taking multiple tissue sections from a tissue block which are subsequently stained using special and immunohistochemical (IHC) stains to identify cell types and disease state. Infrared (IR) spectroscopic imaging is a novel approach to deriving cell type and disease status information in an entirely label-free non-perturbing approach from a single unstained tissue section based on the inherent biochemistry of the tissue.

Design: We have built the first ever high-resolution IR imaging instrument capable of imaging in a clinical setting at a spatial resolution of 1µm x 1µm. Previous results demonstrated accurate histological segmentation of breast tissue however this was limited to large cell types. We have imaged at a high-resolution a training array consisting of 50 patient biopsies and a validation array of 50 patient biopsies, with tissues including normal, hyperplasia, dysplasia and cancer. A Bayesian classifier was built to accurately segment the IR data into over ten epithelial and stromal cell types from a single unstained biopsy.

Results: Accurate histological segmentation from an IR image was performed for epithelial and stromal cell types, including epithelial cells, fibroblasts, cancer-activated fibroblasts, lymphocytes, collagen and necrosis. This study also demonstrated for the

first time the identification, chemical characterization, and classification of myoepithelial cells and endothelial cells in breast tissue biopsies using IR imaging. IR spectroscopic imaging coupled with Bayesian classifiers demonstrated a high degree of cell typing accuracy with an Area Under the ROC Curve (AUC) of over 0.9.

Conclusions: IR imaging coupled with spectral classifiers represents a novel approach to derive cell type and disease status information from tissue based on tissue biochemistry without the requirement for staining. IR imaging has the potential to be a powerful adjunct to the current clinical workflow, with the ability to give additional information about cell types present without requiring additional analysis. In addition, IR imaging has the potential to give insight into chemical changes associated with breast cancer progression.

2093 Identification of Biochemical Changes Associated with Diabetes in Renal Glomeruli by Infrared Spectroscopic Imaging

MJ Walsh, S Setty, A Kajdacsy-Balla, R Bhargava. University of Illinois at Urbana-Champaign, Urbana, IL; University of Illinois at Chicago, Chicago, IL.

Background: The ability to detect chemical changes in tissues is limited by the level of resolution of special stains and immunostains. Infrared (IR) spectroscopic imaging has shown great promise at measuring biochemical changes in tissues in an entirely label-free fashion. Renal changes in diabetes as seen by light and electron microscopy include expansion of the glomerular mesangium and glomerular and tubular basement membranes by deposition of matrix thus leading to chronic renal failure. IR spectroscopic imaging has the potential to allow for novel insight into the biochemical changes in diabetes including non-enzymatic glycosylation of matrix proteins and altered composition of the matrix.

Design: 16 kidney biopsies were acquired, 8 from non-diabetics and 8 from diabetics were analyzed. A formalin-fixed paraffin-embedded serial section was stained using Periodic Acid Schiff and an adjacent unstained tissue section were obtained. IR images were acquired of the whole tissue at a low resolution (6.25x6.25microns) for the identification of gross chemical changes observed between normal and diabetic patients. In addition, high resolution IR images were acquired glomeruli and proximal tubules. Regions within the glomeruli were categorized as normal mesangium, early Kimmelstiel-Wilson (KW) nodules, late KW nodules, glomerular basement membranes and other areas from obsolescent glomeruli and spectroscopic data extracted for comparison.

Results: New high resolution IR imaging techniques have allowed for the visualization and chemical characterization of glomerular structures in kidney tissues, including glomerular basement membrane, mesangium and Bowman's capsule. Chemical changes measured by IR were found to be different in normal and diabetic tissues, in particular, increased levels of glycosylation in late KW nodules of the mesangium as compared to the mesangium from normal subjects.

Conclusions: IR spectroscopic imaging can allow for novel insight into the chemical changes occurring in kidney tissue structures that correlate with disease states. In particular, this work demonstrates increasing levels of glycosylation can be measured using IR imaging in an entirely label-free fashion. Future work will focus on the identification of pre-diabetic changes and whether predictions of increasing glycation and extracellular matrix composition can be related to early pre-diabetes before the appearance of histological changes.

2094 Slide-to-Slide Arrays for High-Throughput Molecular Profiling or Rare Tumor Specimens

SE Weissinger, P Moller, JK Lennerz. Ulm University, Ulm, Germany.

Background: Tissue microarrays (TMA) have become an important tool in high-throughput molecular profiling of tissue samples in the translational research setting. Unfortunately, high-throughput profiling in small biopsy specimens or rare tumor samples (e.g. orphan diseases) is often precluded due to limited amount of tissue. Here, we present a method that allows construction of TMAs from individual 2-5 µm sections for subsequent molecular profiling.

Design: The slide-on-slide TMA technique requires a series of chemical exposures (xylene-methacrylate exchange) in combination with re-hydrated lifting, microdissection of donor-tissues into multiple small tissue fragments and subsequent re-mounting on separate recipient slides. We assessed efficacy of microdissection and mounting by number of dropouts in re-localized tissues. Quality of downstream analyses was compared with traditional assessment for the following variables: antigen-retrieval, primary antibodies, detection systems, histochemical stains, FISH as well as DNA-extractions.

Results: From a technical perspective, building a slide-to-slide array is quick reliable and cost-effective. The three most important aspects for successful re-localization of tissue sections onto the recipient array are: appropriate case selection, precise microdissection, and exact array mounting. We tested 9 different antigen retrieval techniques in combination with over 50 different antibodies, 6 histochemical stains, 8 different FISH probe-sets and several PCR-based techniques including sequencing, which all functioned appropriately. The number of drop outs ranged from 0.8-6.2%; however, we applied the same slide-on-slide technique successfully to fill these dropouts. H&E assessment of donor slides confirmed a transfer efficacy of over 93%, depending on the size of the tissue (range 76-100%). The presented technique requires manual dexterity; however, when directly compared to skills and investments in equipment and personnel for a functioning TMA facility, the tools and effort to learn and perform the slide-on-slide TMA-technique is trivial.

Conclusions: Here, we present a quick, reliable, and cost-effective method that offers the key advantages of traditional tissue microarrays – even when tissue is sparse. The perspectives of this technology in biomedical sciences are promising given that it allows researchers to create more data with less tissue.

2095 Utility of miR-1 and miR-145 microRNA Probes in Distinguishing Smooth and Skeletal Muscle Differentiation

L Xue, K Kalra, R Pillai, MB Amin, DJ Luthringer. BioGenex Laboratories, Fremont, CA; Cedars-Sinai Medical Center, LA, CA.

Background: Determining specific patterns of differentiation is critical to many aspects of diagnostic pathology, including classification of soft tissue tumors. MicroRNAs (miRNAs) are a group of non-coding RNAs 18-22 base-pairs in length, which play critical roles in a many cellular functions including disease states and cancer. New technology allows miRNA detection by in situ hybridization (ISH) techniques. miR-1 is specifically expressed in adult cardiac and skeletal muscle, and miR-145 is expressed by smooth muscle including bladder, stomach and bowel. The purpose of this study was to explore utility of this evolving technology in the expression of two miRNA probes in hopes that it may find application in solving challenging aspects of tumor differentiation.

Design: Samples of formalin-fixed paraffin embedded (FFPE) tissue were studied, consisting of 3 cardiac muscle, 4 skeletal muscle, 3 colon, 2 small bowel, 2 stomach. Cases were subjected to ISH using FAM-labeled Hsa-miR-1 and Hsa-miR-145 probes (BioGenex) followed by Super Sensitive ISH Detection Kit (BioGenex, DF400-YAX). Slides were heated in Nucleic Acid Retrieval Solution I (NAR-I, BioGenex) for 10 min at 92C, subjected to hybridization buffer for 30 min, incubated with 40 nM of microRNA probe for 60 min at 50 C followed by stringency washes. The signal was amplified with anti-fluorescein antibody and poly-HRP labeled secondary antibody, which can develop brown color with DAB chromogen. Scramble probes served as negative control. Areas of muscle tissue were assessed for chromagen.

Results: In all cases, cardiac, skeletal and smooth muscle cells demonstrated crisp, cytoplasmic staining. Background staining was minimal. Smooth muscle fibers in adjacent blood vessels decorated with chromagen. Scramble (negative controls) probes were non-reactive.

Conclusions: In situ hybridization with probes to specific miRNAs can be utilized in diagnostic pathology. miR-1 and miR-145 probes are capable of marking cardiac, skeletal and smooth muscle tissue in formalin fixed paraffin embedded samples. Application of this technology with muscle specific probes to soft tissue tumors may be useful in determination of differentiation and thus aid in classification.

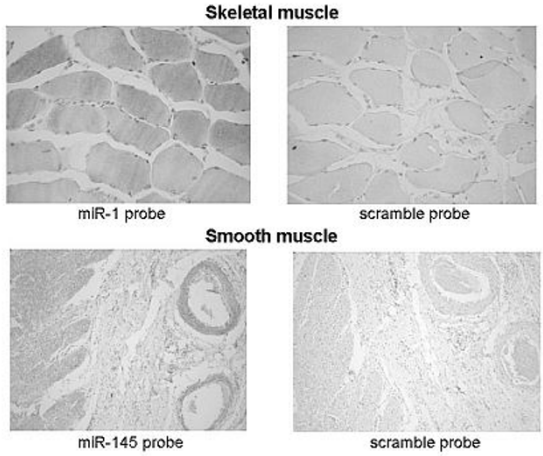

2096 Validation of Tissue Preservation Using a Vacuum Sealed Formalin-Free Transport System

RJ Zarbo, M Dib, RC Varney, BA Jones, N Main. Henry Ford Health System, Detroit, MI.

Background: Formalin fixing and transporting tissue specimens is a process over 100 years old that potentially exposes healthcare workers to toxic, carcinogenic formaldehyde. Formalin spilled in operating room (OR) or laboratory is a health hazard to be contained as a hazardous material. We seek to redesign this work process so formalin is removed from 4 hospitals in the process of transportation of human specimens to an Anatomic Pathology Core Laboratory.

Design: TissueSAFE high vacuum biospecimen transfer system (Milestone Medical, Kalamazoo, MI) was evaluated for vacuum sealed, formalin-free transfer and storage in 3 validations:1) Preservation of surgical specimens vacuum sealed and stored at 4°C and 7°C for 24, 48 and 72 hours compared to paired formalin fixed tissues; 2) Transport and storage of specimens sealed in OR of a community hospital 25 miles away at 4°C for 24 and 48 hours; and 3) Preservation of surgical specimens sealed in FS Room adjacent to 30 ORs then transported at 4°C to the Core Lab within the same hospital, range of storage times 1-10 hours before tissue examination, fixation, processing and histologic assessment. All slides were H+E stained and evaluated by pathologists using a 3 part scale of Acceptable for Diagnosis, Inferior Quality for Diagnosis or Unacceptable for Diagnosis.

Results: SCHEME #1: 9 cases, 7 tissue types (50 blocks): liver, uterus, ovary, lymph node, leg, lung, fatty pannus. All were Acceptable for Diagnosis except for 4 blocks of liver that were under processed and coded as Inferior Quality for Diagnosis. **SCHEME #2:** 9 cases, 8 tissue types (56 blocks): stomach, gallbladder, placenta, fallopian tube, uterus, thyroid, bowel, fistula. All were Acceptable for Diagnosis by histologic evaluation at 1 and 2 days storage under vacuum in the cold. **SCHEME #3:** 30 cases, 16 tissue types, (164 blocks): lung, kidney, stomach, uterus, colon, small intestine, gall bladder, thyroid, brain, tonsil, skin, TURBT, TURP, hemorrhoid, appendix, arterial plaque. All but 2 cases were Acceptable for Diagnosis with 1 TURBT (5 hour storage)

and 1 kidney (2.5 hour storage) deemed Inferior Quality for Diagnosis due to "air-drying" and lack of crisp cytologic tumor detail, respectively.
Conclusions: Vacuum sealed tissues held at 4°C are preserved for histologic assessment when held in that state up to 48 hours. The nature of the 2 histologically inferior exceptions with low storage times require further study. TissueSAFE vacuum transport shows promise to provide a platform for designing formalin-free ORs and transport of tissue specimens to processing laboratories.

2097 *MDM2* Determination by Brightfield Dual Color *In Situ* Hybridization: Interobserver Reproducibility and Correlation with FISH
G Zhang, E Downs-Kelly, C Lanigan, R Tubbs. Cleveland Clinic, Cleveland, OH.
Background: *MDM2* gene amplification is present in approximately 20% of sarcomas. The identification of *MDM2* amplification can serve as an ancillary diagnostic tool especially in the setting of atypical lipomatous tumors /well-differentiated liposarcoma as they characteristically harbor alterations in the 12q13-15 amplicons resulting in amplification of *MDM2;* conversely, lipomas and other histologic mimics lack amplification. We have previously described a brightfield assay (AIMM 2011; 19:54-61) to visualize both *MDM2* and CHR12 within the same tumor nuclei. Using a third generation repeat-free probe set and dual-color, *in situ* hybridization (Dual ISH) brightfield detection assay (VentanaMedical Systems, Inc. Tucson AZ) we assessed interobserver interpretative reproducibility of Dual ISH and correlated Dual ISH with the *MDM2* genotype as determined by fluorescence in situ hybridization (FISH; Abbott Molecular Vysis).
Design: Lipomatous lesions seen in a soft tissue consultative practice were assessed for *MDM2* amplification by both FISH and Dual ISH on consecutive 4 micron whole tissue sections of formalin-fixed and paraffin-embedded tissue. Fluorescent and brightfield microscopy were used respectively with the average number of *MDM2* and CHR12 signals enumerated in the nuclei by quantification of at least 20 nuclei/specimen with a *MDM2*/CHR12 ratio calculated for each case. A ratio of <2.0 was considered non-amplified whereas a ratio ≥ 2.0 was considered amplified, according to previously published criteria. Cases with endogenous signal present in endothelial cells or fibroblasts were considered scorable and were scored independently by two reviewers; correlation between observers and FISH was assessed.
Results: Of the 56 cases assayed, FISH and Dual ISH had complete concordance (100%) with 16 cases identified as *MDM2* amplified and 40 cases identified as *MDM2* non-amplified. Agreement between observers (EDK and RRT) was similarly excellent with all scored cases being concordant.
Conclusions: Brightfield Dual ISH assessment of *MDM2* gene status has excellent correlation with FISH and is reproducible among reviewers. This assay offers the advantage of brightfield microscopy which allows for the assessment of tissue morphology which can be extremely helpful in cases where atypical/neoplastic nuclei are limited.

Ultrastructural

2098 Neuroendocrine Tumors of Cervix – Clinical, Morphologic, Immunophenotypic, and Electron Microscopic Features in Two Cases
B Assylbekova, S Billah, S Kolodziej, M Bhattacharjee. University of Texas Medical School at Houston, Houston, TX.
Background: Neuroendocrine tumors of the uterine cervix are rare in the gynecologic tract. The most recent Surveillance, Epidemiology and End-Results data on neuroendocrine tumors of the uterine cervix reported incidence of 0.42 cases per 1,000,000 women. They are being increasingly recognized with the more routine use of immunostaining in the evaluation of histopathologic features suggesting neuroendocrine differentiation. They can be a pure lesion or occur in combination with adenocarcinoma or squamous cell carcinoma. Analogous to lung neuroendocrine tumors, cervical tumors are classified in four groups that are carcinoid, atypical carcinoid, large cell neuroendocrine tumors and small cell carcinoma. The former are grouped with the neuroendocrine tumors, whereas the latter are categorized as neuroendocrine carcinomas (NECs).
Design: We report the clinical and complete pathologic features in two such cases. The patients were 48 and 71 y and presented with vaginal bleeding. Both were multiparous females; both had history of hypertension and one was a smoker. Direct examination, and imaging studies revealed large cervical/lower uterine masses with obvious pelvic lymphadenopathy in one. The tumors ranged from 3.5 and 11.3 cm.
Results: Biopsies and hysterectomy specimens showed prominent neuroendocrine features by conventional morphology, with inconsistent immunostaining results; focal adenocarcinoma features were seen in one case. Transmission electron microscopy showed poorly differentiated cells with large nuclei with dispersed heterochromatin, prominent nucleoli, and occasional cytoplasmic dense-core granules. No cytoplasmic intermediate filaments were seen. Focally, luminal intercellular junctions were seen in the case with focal adenocarcinomatous features.
Conclusions: Recognition of NECs is important for appropriate therapy and management since these patients have worse clinical outcomes when compared with conventional cervical squamous or adenocarcinomas. Immunohistochemistry may be inconclusive in determining neuroendocrine differentiation, and should be supplemented with ultrastructural studies for confirmation and correct categorization of the carcinoma for appropriate management.

2099 TTF-1 Associated Surfactant Deficiency: Role of Ultrastructural Evaluation
J Hicks, G Mierau, E Wartchow, C Langston. Baylor College of Medicine & Texas Children's Hospital, Houston, TX; Children's Hospital Colorado, Aurora, CO.
Background: Defects in *NKX2-1* gene (14q13-21) encodes thyroid transcription factor-1 (TTF-1) and results in Brain-Thyroid-Lung Syndrome (MIM 610978), characterized by benign hereditary chorea, hypotonia, ataxia, congenital hypothyroidism and respiratory disease. TTF-1 is a critical factor in type II pneumocyte differentiation. In addition, surfactant protein synthesis is dependent on TTF-1. Deficiency of TTF-1 leads to a congenital surfactant deficiency syndrome that may be mistaken for Surfactant A, B, C or ABCA3 deficiency.
Design: Pathology archives of 2 pediatric hospitals identified 6 neonates, infants and young children (3F:3M, age range 6 mos to 3 yrs) with severe respiratory disease that lead to lung biopsy and/or subsequent lung transplantation. Clinical features were variable with some presenting in infancy with respiratory distress syndrome and others presented in early childhood with gradual onset of respiratory insufficiency, hypoxemia, failure to thrive and interstitial lung disease. Lung biopsies were performed and evaluated by routine histologic and electron microscopic (EM) techniques.
Results: Lung biopsies and explants showed features of chronic pneumonitis of infancy, lipoid pneumonia and cholesterol pneumonia. There was alveolar wall widening with prominent alveolar epithelial hyperplasia and increased interstitial cells with mild chronic inflammation and mild interstitial fibrosis. There was hyperplasia and interlobular extension of smooth muscle cells. PAS positive globules, macrophages, eosinophils and cholesterol clefts were seen in alveolar spaces. Abnormal growth development was present, characterized by decreased alveolar density, and poorly subdivided and enlarged airspaces. EM showed relatively normal lamellar bodies with infrequent disorganized lamellar bodies with concentric phospholipid membranes and eccentric dense cores. The features were those typically associated with surfactant deficiency, with exclusion of Surfactant B and ABCA3 Deficiency from consideration.
Conclusions: Discovery of features of surfactant deficiency that may be associated with TTF-1 deficiency on lung biopsy is often the first indicaton that a child may have Brain-Thyroid-Lung Syndrome secondary to *NKX2-1* gene mutation. Ultrastructural examination in these cases is important in eliminating Surfactant B and ABCA3 Deficiencies from consideration based upon ultrastructural features of lamellar bodies. EM findings may guide appropriate genetic testing for the specific mutation responsible for the child's underlying respiratory disease.

2100 Avoiding Pitfalls in Ultrastructural Evaluation of Peripheral Blood Leukocyte Buffy Coats for Metabolic Inclusion Disease
J Hicks, E Wartchow, G Mierau. Baylor College of Medicine & Texas Children's Hospital, Houston, TX; Children's Hospital Colorado, Aurora, CO.
Background: Ultrastructural examination of leukocytes within buffy coats prepared from peripheral blood samples is often performed in diagnostic electron microscopy laboratories for evaluation in children with suspected metabolic inclusion disease. Identification of characteristic inclusions by electron microscopy can guide appropriate metabolic disease genetic testing. There are certain ultrastructural features that may be misinterpreted as metabolic inclusions and result in a possible misdiagnosis.
Design: The pathology archives of a pediatric hospital were accessed over a 5 year period to identified ultrastructural inclusions in leukocytes from buffy coats that mimic metabolic disease inclusions and represent potential pitfalls in diagnosis. Buffy coats from 35 patients were identified as having ultrastructural inclusions that possess ultrastructural inclusions that mimic metabolic disease inclusions. The majority of the children were under 2 years of age (75%) with an age range from 1 month to 7 years, and had clinical signs and symptoms concerning for metabolic inclusions diseases (most commonly neuronal ceroid lipofuscinosis [NCL]).
Results: Analysis of the electron microscopic digital images revealed 3 types of inclusions that may mimic metabolic inclusion disease. The most common was tubular arrays within the cytoplasm of lymphocytes (22/35). These tubular arrays may mimic certain forms of NCL; however, the tubular arrays are typically associated with natural killer cells (NK cells). Tubular reticular inclusions (TRIs)were identified in 9 cases. TRIs are associated with autoimmune disease (systemic lupus erythematosus), immunocomprised and immunosuppressed states, and viral infections. Myelin figures were seen in 12 cases, sometimes in cases also with tubular arrays and TRIs. These figures represent degradation products of cell and cytoplasmic membranes.
Conclusions: Identifying cytoplasmic inclusions in peripheral blood leukocytes that may mimic metabolic inclusion disease is important to avoid misdiagnosis of children with suspected metabolic disease and avoidance of unnecessary, inappropriate and expensive genetic testing, Ultrastructural examination of peripheral blood leukocytes in buffy coats provides an initial screening process that assists the clinician in decision making in selecting definitive diagnostic tests.

2101 Odontogenic Myxoma: Review of Histopathologic, Immunocytochemical and Ultrastructural Features
J Hicks, R Laucirica, C Finch, J Bouquot. Baylor College of Medicine, Houston, TX; University of Texas Houston School of Dentistry, Houston, TX.
Background: Odontogenic myxomas arise from odontogenic ectomesenchyme and involve the mandible and maxilla. Most are located in the mandible (two-thirds). There is a wide age range, with an average age of 25 to 30 years. The typical tumor is asymptomtic with painless jaw expansion, and found incidentally during dental examination. Diagnostic imaging may reveal a unilocular, multilocular or soap bubble lesion, displacing and/or resorbing teeth. The tumor is not encapsulated, infiltrates bone and may require aggressive curettage.